



Tidal restriction likely has greater impact on the carbon sink of coastal wetland than climate warming and invasive plant

Pan Zhou · Siyuan Ye · Liujuan Xie · Ken W. Krauss · Lixin Pei · Samantha K. Chapman · Hans Brix · Edward A. Laws · Hongming Yuan · Shixiong Yang · Xigui Ding · Shucheng Xie

Received: 28 March 2023 / Accepted: 5 July 2023 / Published online: 29 July 2023
© The Author(s), under exclusive licence to Springer Nature Switzerland AG 2023

Abstract

Aims Coastal salt marshes are productive ecosystems that are highly efficient carbon sinks, but there is uncertainty regarding the interactions among climate warming, plant species, and tidal restriction on C cycling.

Methods Open-top chambers (OTCs) were deployed at two coastal wetlands in Yancheng, China, where native *Phragmites australis* (*Phragmites*) and

invasive *Spartina alterniflora* (*Spartina*) were dominant, respectively. Two study locations were set up in each area based on difference in tidal action. The OTCs achieved an increase of average daytime air temperature of ~1.11–1.55 °C. Net ecosystem CO₂ exchange (NEE), ecosystem respiration (R_{eco}), CH₄ fluxes, aboveground biomass and other abiotic factors were monitored over three years.

Results Warming reduced the magnitude of the radiative balance of native *Phragmites*, which was determined to still be a consistent C sink. In contrast, warming or tidal flooding presumably transform the *Spartina* into a weak C source, because either warming-induced high salinity reduced the magnitude of

Responsible Editor: Zucong Cai.

Supplementary information The online version contains supplementary material available at <https://doi.org/10.1007/s11104-023-06160-x>.

P. Zhou · S. Xie
School of Earth Sciences, China University of Geosciences (Wuhan), Wuhan 430074, China

P. Zhou · S. Ye · L. Xie · L. Pei · H. Yuan · S. Yang · X. Ding
Laboratory for Marine Geology, Laoshan Laboratory, Qingdao 266237, China

P. Zhou · S. Ye · L. Pei
Chinese Academy of Geological Sciences, Beijing 100037, China

P. Zhou · S. Ye (✉) · L. Xie · L. Pei · H. Yuan · S. Yang · X. Ding
Key Laboratory of Coastal Wetlands Biogeosciences, Qingdao Institute of Marine Geology, China Geological Survey, Qingdao 266237, China
e-mail: siyuanye@hotmail.com

P. Zhou · S. Ye
Institute of Marine Science and Technology, Shandong University, Qingdao 266237, China

K. W. Krauss
U.S. Geological Survey, Wetland and Aquatic Research Center, Lafayette, LA 70506, USA

S. K. Chapman
Department of Biology and Center for Biodiversity and Ecosystem Stewardship, Villanova University, Villanova, PA 19085, USA

H. Brix
Department of Bioscience, Aarhus University, Aarhus C 8000, Denmark

NEE by 19% or flooding increased CH₄ emissions by 789%. Remarkably, native *Phragmites* affected by tidal restrictions appeared to be a consistent C source with the radiative balance of 7.11–9.64 kg CO₂-eq m⁻² yr⁻¹ because of a reduction in the magnitude of NEE and increase of CH₄ fluxes.

Conclusions Tidal restrictions that disconnect the tidal hydrologic connection between the ocean and land may transform coastal wetlands from C sinks to C sources. This transformation may potentially be an even greater threat to coastal carbon sequestration than climate warming or invasive plant species in isolation.

Keywords NEE · R_{eco} · CH₄ fluxes · Radiative balance · Carbon source/sink · Coastal wetlands

Abbreviations

OTCs	Open-top chambers
NEE	Net ecosystem CO ₂ exchange
R_{eco}	Ecosystem respiration
C	Carbon
SGWP	Sustained-flux global warming potential
SGCP	Sustained-flux global cooling potential
GHG	Greenhouse Gas
GPP	Gross primary production
AGB	Above ground biomass
WTD	Water table depth
CROWNs	Coastal-wetland Research On Warming Networks
UGGA	Ultra-Portable Greenhouse Gas Analyzer
OMS	Online monitoring systems
TC	Total C
SOC	Soil organic C
TN	Total nitrogen
CI	Confidence interval (95%)
Fe	Iron
Zn	Zinc
Cu	Copper
CIA	The chemical index of alteration

E. A. Laws
Department of Environmental Sciences, School
of the Coast and Environment, Louisiana State University,
Baton Rouge, LA 70803, USA

Introduction

Coastal wetlands are very efficient in capturing and storing carbon. The area of coastal wetlands is less than 0.5% that of the ocean, but the carbon (C) stored therein accounts for about 50% of the total organic C buried in marine sediments (Duarte et al. 2005). The atmospheric carbon sequestered in vegetated, tidally influenced coastal ecosystems has been termed “Blue Carbon” (Nellemann et al. 2009). Blue carbon wetlands represent one of the densest C sinks in the biosphere (Duarte et al. 2013) because of (1) the high efficiency with which wetlands trap suspended matter and associated organic C during tidal inundation and sedimentation induced by riverine flooding, (2) the appreciable rates of belowground plant root growth in wetlands, and (3) lower concentrations of oxygen in wetland soils than in upland counterparts. Metabolism dominated by anaerobic decomposition reduces the rate of soil organic matter mineralization in wetlands. Furthermore, the sulfate ions (SO₄²⁻) in seawater that inundates coastal wetlands inhibit the production of methane (CH₄) (Capooci et al. 2019; Poffenbarger et al. 2011). The carbon captured by coastal wetlands can therefore be stored in soil or sediment for thousands of years (Lo Iacono et al. 2008; Macreadie et al. 2013; McKee et al. 2007). Methane has a greater sustained-flux global warming potential (SGWP) (Neubauer and Megonigal 2015) than CO₂. The high C sequestration rates and low rates of CH₄ emissions that distinguish coastal wetlands as C sinks limit the effect that Greenhouse Gas (GHG) emissions have on Earth’s radiative balance (Chmura et al. 2003; Neubauer and Megonigal 2021).

However, the lifetime of the organic C stored in wetland soils depends on the form and location of the stored C (Angst et al. 2017; Ravn et al. 2020; Rumpel and Kögel-Knabner 2011), the environmental conditions in the soil (Chapman et al. 2019), and the presence of microenvironments suitable for decomposers and detritivores (Barthod et al. 2020). Furthermore, the decomposition of C and the uptake of C in wetlands are interrelated processes. Lu et al. (2020) has revealed that the decomposition of organic matter in coastal wetland stimulates plant growth and enhances the absorption of atmospheric C through the acceleration of weathering and the subsequent release of mineral nutrients. The interaction between plant growth and mineral weathering, along with the underlying

mechanisms that connect organic matter decomposition and carbon uptake, are susceptible to anthropogenic alterations such as climate warming, invasive plant species, and tidal limitation (Chen et al. 2015; Mueller et al. 2016; Noyce and Megonigal 2021). These changes can confound accurate prediction of future alterations of radiation balance in coastal wetlands.

An increase in temperature can alter soil biogeochemical reactions. When the temperature of a body of water rises, for example, the solubility of CO₂ in the water decreases, and some of the CO₂ dissolved in the water escapes into the atmosphere (Li 2016). Furthermore, temperature indirectly affects the exchange of GHGs in coastal wetlands by controlling the rates of microbial metabolism and plant growth (Chapman et al. 2021; Noyce and Megonigal 2021). Warming can enhance gross primary production (GPP) by prolonging the growing season, increasing plant biomass, and enhancing plant photosynthetic performance (Yu et al. 2018). However, warming can also increase the rate of ecosystem respiration (R_{eco}) and therefore stimulate emissions of CO₂ and CH₄ associated with the mineralization of organic C by enhancing the respiration rates of both autotrophs and heterotrophs. Excessive warming may adversely affect rates of carbon fixation by wetland plants if temperatures become supraoptimal.

In contrast to native plant species, the impacts of invasive plants are difficult to predict because they are function of ecological and geological conditions. The impacts may lead to an increase of carbon sequestration (Ge et al. 2015; Liao et al. 2007; Liu et al. 2022) or a transition from sink to source (Bradley et al. 2006; Xu et al. 2022). The invasion of new and prolifically growing plant species within saltmarshes has led to enhanced C pools in some ecosystems via, inter alia, increases of aboveground biomass (AGB) (Bottollier-Curtet et al. 2013). However, other studies have indicated that plant invasion leads to a release of a large amount of C-based greenhouse gases (Tong et al. 2012; Zhou et al. 2015), and still other studies have suggested that a transition from native to non-native species may have a limited net influence (Wang et al. 2019). At least two lines of reasons account for these conflicting results. First, the feedback effects of invasive plants differ significantly as a function of the eco-geological conditions that characterize specific

soil environments (Davidson et al. 2018). Second, measurements made in many studies have emphasized only a certain component of the C cycle and have failed to include all relevant fluxes, i.e., NEE, R_{eco} , and CH₄ fluxes. Integrating the impacts of biotic factors such as invasive plant species with abiotic changes like warming is essential to advancing our understanding of future coastal wetland C cycling.

Tidal restriction refers to the limitation or obstruction of ocean-land interaction of coastal wetlands caused by human activities that alter the structure or landform of the area. Tidal restriction, such as dams and roads, have seriously affected the carbon sink of coastal wetlands (Kroeger et al. 2017). This has resulted in a reduction of carbon sequestration and an increase of GHG emissions (USEPA 2020). For example, reclamation-induced tidal restriction can increase the composition of dissolved carbon in salt marsh creeks and make them sources of greenhouse gases (Tan et al. 2021). Based on the modeled of climate forcing, Kroeger et al. (2017) have concluded that restoring tidal connectivity has a greater impact on reducing GHG emissions and increasing carbon sequestration than wetland creation or conservation. The growth of wetland plants, the emissions of CO₂ and CH₄, and the balance between the production and decomposition of organic matter largely depend on water table depth (WTD) and salinity. On the one hand, tidal restriction will cause wetland drainage, which exposes organic matter that has accumulated over many years to oxygen. The aerobic decomposition of that organic matter leads to the production of CO₂ (Drexler et al. 2013). On the other hand, tidal restriction can also result in a reduction of salinity and lead to increased CH₄ release due to the lack of SO₄²⁻ as an electron acceptor.

This study aimed to quantify the effects of climate warming, different plant species, and tidal restriction on the carbon cycle in coastal wetlands of Yancheng, China. To achieve this goal, we used Open Top Chambers (OTCs) and selected locations where there were differences between plant habitats and tidal influences. We addressed two key questions: (1) Did climate warming, plant species and tidal restriction change the exchange of GHGs and the radiation balance in these coastal wetlands? (2) Which of these three factors had a greater impact on the carbon cycle of these coastal wetlands?

Materials and methods

Site details

The Yancheng Wetland (32°32′–34°25′ N, 119°55′–121°50′ E) is located in a muddy coastline along the Jianghuai Plain, Jiangsu Province, China (Fig. 1), and is the largest subtropical tidal saltmarsh in China. It has been included in the Ramsar List of International Important Wetlands. The average annual tidal range in the study area is 3–5 m (Ding et al. 2014). Because of the influence of the East Asia Monsoon and the plain landform, Yancheng has a warm, humid climate. The mean air temperature is 15.5 °C, and the mean annual precipitation is 1015 mm (Appendix S1: Fig. S1). The dominant saltmarsh vegetation types are *Phragmites australis* and invasive *Spartina alterniflora*. The Yancheng Wetland is a migration hub for over 400 species of migratory birds; more than 50 million migratory birds visit it annually (Ye et al. 2021). Sustainable management priorities include provision of wetland services, which include enhanced CO₂ sequestration and provision of a habitat for birds (Ye et al. 2021).

Two experimental warming sites were studied, both of which are part of the Coastal-wetland Research On Warming Networks (CROWNs) collaboration. This collaboration was established in early 2018 on the northeastern coast of China with partner sites in the United States and Europe.

Experimental design

Table S1 summarizes conditions at two of the experimental sites. The CROWN-S site was the Simaoyou *Spartina* wetland in the south of Yancheng and was divided into two locations, a warming-experimental location (CROWN-SW) and an alternate control location (CROWN-SA). The CROWN-SA was located 2 km away from the CROWN-SW and provided an opportunity to examine the response of GHG fluxes to differences between environmental conditions other than temperature. The CROWN-SA was more strongly affected by tides than the CROWN-SW (Fig. 1). The CROWN-P site was vegetated by native *Phragmites*. It was 60 km to the north of the CROWN-S and also included two locations, a warming-experimental location (CROWN-PW), and an alternate control location (CROWN-PA). The

CROWN-PA was located 2 km southwest of the CROWN-P (Fig. 1). Unlike the CROWN-PW, the CROWN-PA had no apparent exchange with the sea because of a road that blocked tidal exchange.

The experimental studies spanned 29 months from May 2018 to September 2020. Open-top chambers (OTCs) were installed to produce continuous, passively warmed environments for *Spartina* and *Phragmites* (Fig. 1). The OTCs were designed as large, octagonal structures for wind resistance and were 2.7 m tall with eight 1.07-m-wide, clear, side panels (maximum within-chamber diagonal distance of 2.8 m). Each chamber occupied a ground area of 5.53 m². The frames of the OTCs were made of aluminum alloy. The tempered-glass panels were 4 mm thick with light transmittance >92% to ensure sufficient oblique solar radiation. The tops were open. A 10-cm vertical space was reserved between the bottom of the OTC and the soil surface to accommodate the dynamic astronomical and wind tides, as well as flooding caused by rainfall. Next to each warming plot, a non-warming control plot with the same octagonal base was installed, but without OTCs. OTCs were also not installed at the two alternate control locations, CROWN-SA and CROWN-PA. Each warming-experimental location included 6 warming plots (wCROWN-SW or wCROWN-PW) and 6 non-warming control plots (cCROWN-SW or cCROWN-PW), and each alternate control location included 6 alternate control plots without OTCs (cCROWN-SA or cCROWN-PA) (Appendix S1: Table S1). Online monitoring systems (OMS) were installed within one of the 6 warming plots and one of the 6 non-warming control plots at each of CROWN-SW and CROWN-PW (Appendix S1: Table S1). Boardwalks (width > 30 cm) were installed at all four of the locations to prevent investigator trampling during monitoring (Yu et al. 2022).

Gas flux measurements

Measurements of NEE, R_{eco} and CH₄ fluxes were made using an Ultra-Portable Greenhouse Gas Analyzer (UGGA) (Los Gatos Research, Quebec, Canada) coupled with a static chamber. The cylindrical static chambers were made of clear plexiglass (50 cm in diameter, 50 cm in height). Vent holes were provided on the side of the chamber to connect the UGGA to monitoring instruments. Each chamber was set on a

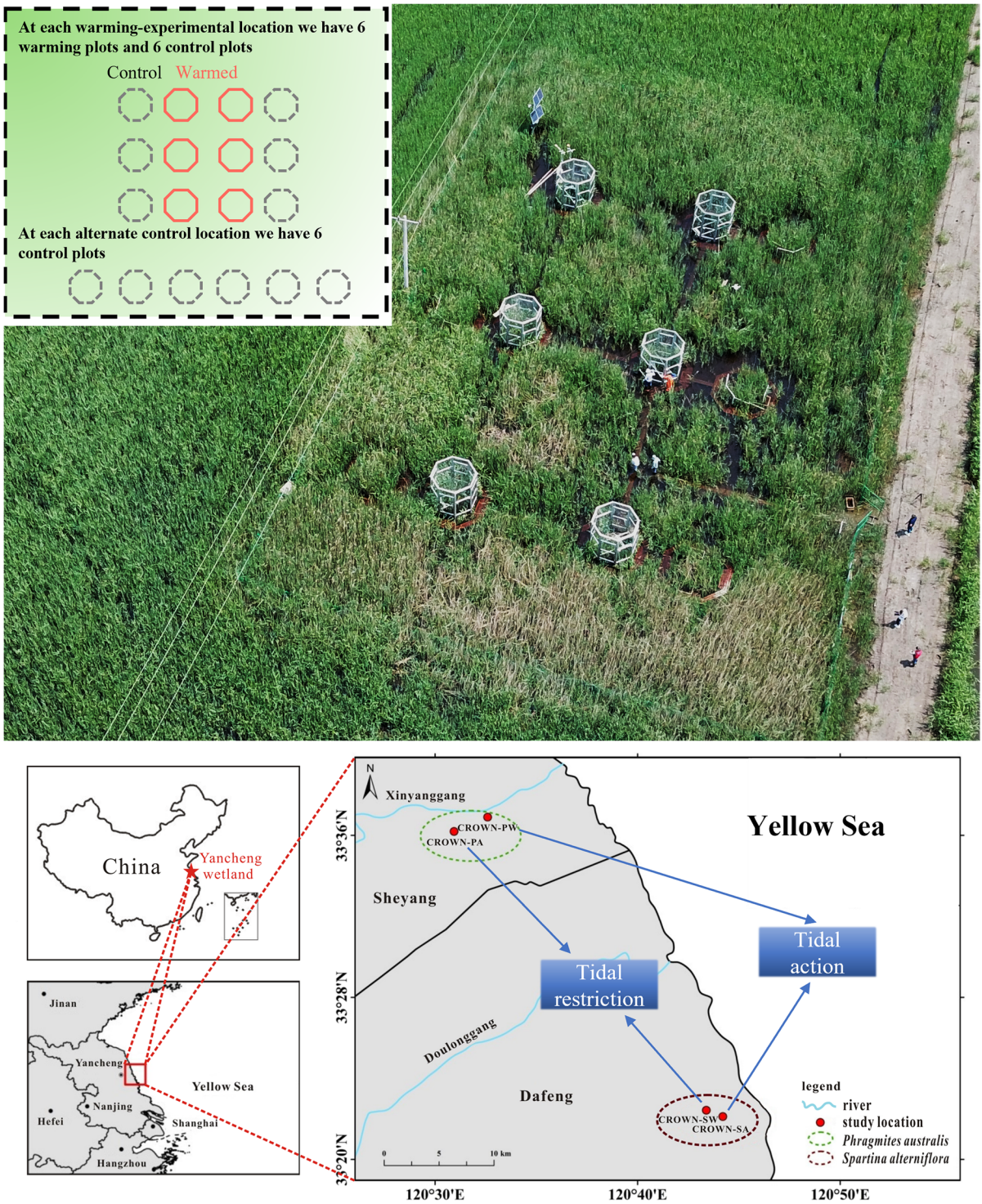


Fig. 1 Experimental design (upper panel) and locations in the *Spartina alterniflora* and *Phragmites australis* wetlands in Yancheng (lower panel), Jiangsu Province, China

perennially installed stainless-steel observation base with a trough around the base for chambers to create a water seal. Holes were drilled on the observation base at the soil surface to allow for flood water exchange during non-monitoring periods but were plugged with rubber stoppers during sampling.

The 50-cm chambers were stackable to ensure that plants were overtopped during measurements. Chamber junctions were sealed, and volume adjustments were incorporated based on number of chamber segments needed. A small fan was installed in the chamber at the top to ensure that the gas in the chamber remained fully mixed during UGGA measurements. The UGGA was connected to the chamber, and changes of CO₂ and CH₄ gas concentrations in the chamber were recorded over multiple periods of 3 min. The NEE and CH₄ fluxes were measured directly with light chambers; the measurement of R_{eco} was made with chambers that were darkened by covering them with a blackout cloth. Flux was calculated as follows:

$$F = \frac{dc}{dt} \frac{M}{V_0} \frac{P}{P_0} \frac{T_0}{T} V \quad (1)$$

where F is the gas flux (mg/(m²·h)); dc/dt is the rate of change of gas concentration in the chamber (ppm/sec); M is the molecular weight of the gas (CO₂: 44 g/mol, CH₄: 16 g/mol); P is barometric pressure (hPa) in the chamber; T is the air temperature in the chamber (°C); V is the chamber volume (cm³); T_0 , P_0 and V_0 are gas temperature, barometric pressure and molar volume under standard conditions, respectively.

The measurements were conducted during three growth seasons and are summarized in Table S2: 2018 (May 16 to November 19), 2019 (April 8 to November 2) and 2020 (May 29 to September 16). We were not able to measure gas fluxes at the end of the 2020 growing season due to COVID-19 restrictions. We monitored both sites in the shortest possible time, usually within one week. The measurements were carried out on each plot in turn between 8:30 AM and 4:30 PM.

Environmental parameters

Environmental data were collected and recorded using an online monitoring system (OMS). Parameters measured by the OMS included air temperature

at 100 cm above the ground, soil temperature at 5 cm below the soil surface, and water table depth (WTD) relative to the soil surface. The time step was 10 min. The following sensors were used: for air temperature and relative humidity, a temperature-and-relative-humidity probe (model HMP155A, Vaisala, Finland); for soil temperature, conductivity, and soil moisture content, a soil moisture–conductivity-temperature sensor (model CS655-L, Campbell Scientific, USA); for WTD, a pressure transducer (model CS456, Campbell Scientific, USA). All data were converted to daily averages for subsequent analyses.

At alternate control locations without any OMS installations, we collected environmental data manually at the time of each field monitoring. Briefly, the air temperature was obtained from UGGA when measured gas flux, salinity was tested by pen salinity meter (SA287, HAZFULL, China), and WTD was measured in a piezometer by using water level data logger (MX2001-01, HOBO, the U.S.).

Field sampling and analyses

Soil samples were collected for moisture content, determination of bulk density, and elemental analysis from all six types of two sites (Fig. 1 and Appendix S1: Table S1). Soil surface samples were collected at 3 randomly selected combinations out of 6 plots for each type. We sampled in April, July, September, and November of 2019. Before sampling soils, plant litter on the soil surface was gently scraped with stainless steel tools. Surface soil samples were collected in situ using a weighted metal ring knife (60.35 cm³). The samples were transported to the laboratory and dried to constant weight at 105 °C. After re-weighing, moisture content and bulk density were calculated as follows (Ye et al. 2015):

$$\omega = \frac{m_w}{m_s + m_w} \times 100\% \quad (2)$$

$$\rho_b = \frac{m}{V(1 + \omega)} \quad (3)$$

where ω is the moisture content (%); m_w and m_s are the mass of water (g) in the soil sample and the mass of dry soil (g) in the soil sample, respectively. ρ_b is the bulk density; m is the wet sample mass inside the ring knife (g); and V is the volume of ring knife (cm³).

Soil samples for elemental analysis were randomly selected from 5 sub-samples at each plot, and then mixed into one sample. The samples were wrapped and labeled in tin foil and stored in the refrigerator until laboratory analysis. Total C (TC), soil organic C (SOC) and total nitrogen (TN) measurements were made with an elemental analyzer (Vario, Max CN, Elementar, Germany) (Liu et al. 2017). Major soil elements (P, K Mg, Ca, Fe and Mn) were analyzed using X-ray fluorescence spectroscopy (ZSX Primus II, Rigaku, Japan) (Zhao et al. 2018). Soil trace elements (Zn, Cu) were analyzed using an ICP-MS (820-MS, Varian, the U.S.) (Ding et al. 2019).

The pH and salinity of pore water were measured in the field with an ultra-portable pH meter (6010 M, JENO, the U.S.) and pen salinity meter (SA287, HAZFULL, China), respectively. The concentration of SO_4^{2-} was measured using ion chromatography (ICS-600, Thermo Scientific, the U.S.). Pore water salinity and pH measurement were synchronized with GHG monitoring over three years. Pore water required for testing SO_4^{2-} was collected in April and October 2021.

The chemical index of alteration (CIA) has been used to reflect the extent to which feldspar has weathered to clay minerals (Nesbitt and Young 1982). We used the following formula to determine CIA values:

$$\text{CIA} = [\text{n}(\text{Al}_2\text{O}_3)/(\text{n}(\text{Al}_2\text{O}_3)+\text{n}(\text{Na}_2\text{O})+\text{n}(\text{K}_2\text{O})+\text{n}(\text{CaO}^*))] \times 100 \quad (4)$$

where CaO^* is the CaO incorporated into silicate minerals. The CaO mole numbers were corrected to eliminate the bias caused by the presence of calcium carbonate: $\text{n}(\text{CaO}') = \text{n}(\text{CaO}) - 10 \times \text{n}(\text{P}_2\text{O}_5)/3$; If $\text{n}(\text{CaO}') < \text{n}(\text{Na}_2\text{O})$, then $\text{n}(\text{CaO}^*) = \text{n}(\text{CaO}')$, otherwise $\text{n}(\text{CaO}^*) = \text{n}(\text{Na}_2\text{O})$, where “n” stands for molecular content (McLennan 1993). The CIA was used to classify weathering levels as follows: unweathered ($\text{CIA} < 50$), primary weathering ($\text{CIA} = 50\text{--}64$), moderate weathering ($\text{CIA} = 65\text{--}85$), and intense weathering ($\text{CIA} > 85$).

Above-ground plant biomass measurements

Above-ground biomass was estimated using a non-destructive method (Ye et al. 2016). The heights and basal diameters of all shoots within the observation bases inside the OTC and control frames were measured using a tape measure and a vernier caliper,

respectively. To establish a regression equation for biomass determination within the observation bases, we harvested 30 shoots encompassing the range of heights, diameters and weight outside the observation bases inside the OTC and control frames. Six shoots were dried at 65 °C for 24 h to obtain plant moisture content, which was used to calculate the dry weight of 30 shoots. We used a deformed combination form of the logistic curve to describe the relationship between the dry weight of shoots, heights and basal diameter as follows:

$$W_f = \frac{D_{\max}}{1 + e^{-k_1(D-d_m)}} + \frac{H_{\max}}{1 + e^{-k_2(H-h_m)}} \quad (5)$$

where W_f is the dry weight (g) of each shoot, D is its basal diameter (mm), and H is its height (cm). The parameters D_{\max} , k_1 , d_m , H_{\max} , k_2 , and h_m were determined by least squares. We estimated the areal biomass (g/m^2) inside the frames by substituting the base diameter and height of all the shoots within a frame into Eq. (5), summing the AGB of all shoots, and dividing this sum by the base area.

The period of monitoring the heights, diameters, and weights used to estimate AGB were synchronized with the period of gas monitoring. The heights and basal diameters of the 28 tallest plants were selected only in May and September 2020 to represent the plant traits at the beginning and end of the growing season.

Annual greenhouse gas flux estimation and radiative balance calculation

To estimate daily GHG exchange fluxes, we assumed NEE to be constant throughout the daytime (12 h) and the fluxes of R_{eco} and CH_4 fluxes to be constant throughout the day and night (24 h). The seasonal variation of GHG exchange fluxes was assumed to have a Gaussian distribution. The interannual climate conditions in 2018, 2019 and 2020 were similar (Appendix S1: Fig. S1). The daily GHG exchange fluxes of the years 2018 (5 measurements), 2019 (4 measurements), and 2020 (2 measurements) were combined as one year in the Gaussian model equation:

$$f(x) = a1e^{(-(x-b1)/c1)^2} \quad (6)$$

where $f(x)$ is GHG exchange flux ($\text{mg}/(\text{m}^2\cdot\text{d})$) on day x of the year, and $a1$, $b1$, and $c1$ are parameters.

The parameters a_1 , b_1 , c_1 were determined by least squares after eliminating the abnormal GHG exchange fluxes that were outside the 95% prediction bands of the fitted curve. According to Eq. (6), the flux values of GHG exchange were computed on a daily basis and subsequently aggregated to derive the annual GHG exchange flux.

The CO₂-equivalent GHG fluxes of CO₂ and CH₄ were quantified in terms of their sustained-flux global warming potential (SGWP) if the fluxes were positive (soil/plant-to-atmosphere) or their sustained-flux global cooling potential (SGCP) if the fluxes were negative (atmosphere-to-soil/plant) (Neubauer and Megonigal 2015). Over 100-year time horizons, the SGWP and SGCP of CH₄ is 45 times that of CO₂ on a mass basis (Neubauer and Megonigal 2019). We used NEE and R_{eco} to represent daytime and night CO₂ exchange, respectively. However, R_{eco} was measured during the daytime. We therefore assumed that the actual R_{eco} at night was between zero and the R_{eco} at the daytime (0.5×total R_{eco} 24-hour estimated value), because R_{eco} at night is generally lower than that at daytime (Xu et al. 2017; Yang et al. 2018). The net CO₂-equivalent GHG flux is represented by radiative balance (Neubauer 2021) as follows: where a is a parametric variable. The value of a is zero if R_{eco} is assumed to be zero at night, and the value of a is 0.5 if R_{eco} is constant throughout the day (24 h). When the radiation balance exceeds zero, the type is a C source; when the radiation balance is negative, the type is a C sink.

Statistical analysis

If the data were heteroscedastic, Kruskal-Wallis tests were used to test for differences among types. For AGB and GHG, the effects of experimental warming (wCROWN-SW vs. cCROWN-SW or wCROWN-PW vs. cCROWN-PW), plant species (cCROWN-SA vs. cCROWN-PW) and tidal restriction (cCROWN-SW vs. cCROWN-SA or cCROWN-PW vs. cCROWN-PA), were analyzed by one-way analysis of variance (ANOVA). Paired t -tests were used to analyze whether warming had a significant effect on GHG fluxes. Pearson correlation coefficients were used to analyze whether the correlation between greenhouse gas fluxes and environmental factors were significant.

Linear mixed effects models were used to assess the relations among NEE, and R_{eco} and CH₄ fluxes and the environmental factors. The fixed effects

were plant species (categorical variable), air temperature, salinity, WTD and AGB (continuous variables). The random effects were site and plot. The effect of each variable or interaction was evaluated by removing the variable/interaction from the original model and using a likelihood ratio chi-square test for significant differences at the 5% significance level between the original model and the model without the variable/interaction. The original mixed effects model for GHG fluxes took the form:

$$GHGfluxes_i = \beta_{0i} \cdot AGB_i + \beta_1 \cdot Air\ temperature + \beta_2 \cdot Salinity + \beta_3 \cdot WTD + b_1 \cdot (Site) + b_2 \cdot (Plot) + \epsilon_i \quad (7)$$

Where β , b and ϵ_i are the fixed variable coefficient, random variable coefficient and residuals for plant species, respectively. Statistical analyses were performed in SPSS (version 25, IBM Corporation, 1 New Orchard Rd, Armonk, NY 10,504, USS).

Results

Temperature manipulation

OTCs significantly increased average air temperature by 0.69 °C at CROWN-SW ($p < 0.05$) and 0.54 °C at CROWN-PW ($p < 0.05$) compared to control plots over a day-night cycle. The response of air temperature to warming was particularly apparent during the day, when the difference between warmed and control plots averaged 1.55 °C at CROWN-SW and 1.11 °C at the CROWN-PW. However, there was a slight cooling phenomenon at night, when OTCs decreased average air temperature by 0.18 °C at CROWN-SW and 0.04 °C at CROWN-PW (Appendix S1: Table S3, Figs. S2 and S3).

Environmental parameters and plant characteristics

Table 1 summarizes the environmental parameters and plant characteristics at 6 types. Except for the air temperature at 2 warming-experimental sites (Appendix S1: Table S3, Figs. S2 and S3) and salinity and SO₄²⁻ concentration of CROWN-SW (Table 1), warming did not have a significant impact on environmental parameters. Compared with CROWN-PW, CROWN-SW had lower WTD ($p < 0.05$), lower

Table 1 Physical and chemical environmental parameters and plant characteristics (mean±CI) for experimental studies in Yancheng, Jiangsu Province, China

Parameters and characteristics	wCROWN-SW	cCROWN-SW	cCROWN-SA	wCROWN-PW	cCROWN-PW	cCROWN-PA
Water table depth (cm)	-48.31±0.21 A		25.52±0.47 B	16.64±0.18 C		8.68±2.63 D
Moisture content (%)	28.39±1.73 A	30.60±2.08 AC	28.38±0.58 AD	44.77±2.71 B	45.14±3.00 B	65.64±4.68 E
Bulk density	0.73±0.15 A	0.69±0.14 AC	0.74±0.11 A	0.55±0.11 B	0.55±0.09 BC	0.57±0.10 D
Salinity (PSU)	16.93±2.19 A	14.87±2.36 B	17.93±3.07 A	10.77±2.67 C	11.55±2.26 C	1.00±0.37 D
pH	7.12±0.19 A	7.13±0.14 A	7.38±0.21 A	7.19±0.24 A	7.01±0.22 A	6.99±0.13 A
SO ₄ ²⁻ (mg/L)	1063.52±93.27 A	913.61±46.07 B	640.19±15.26 C	258.56±138.07 D	172.68±160.77 D	9.91±9.17 E
Plant height early season (cm)	101.73±2.75 A	93.09±2.83 B	75.00±1.27 C	240.68±9.07 D	215.50±13.14 E	181.61±12.57 F
Plant diameter early season (mm)	8.07±0.85 A	8.70±0.94 A	8.97±0.75 A	7.09±0.46 B	6.30±0.49 C	6.00±0.51 B
Plant height late season (cm)	161.39±5.30 A	143.54±4.45 B	140.86±4.45 B	318.14±16.24 C	258.11±18.52 D	227.64±16.23 D
Plant diameter late season (mm)	8.20±0.80 AB	9.13±0.70 A	7.38±0.40 ABC	6.54±0.40 C	7.38±0.42 B	6.36±0.96 C
TC (%)	2.00±0.16 A	1.98±0.18 A	1.30±0.10 B	3.46±0.22 C	3.39±0.27 C	6.90±0.14 D
SOC (%)	0.55±0.55 A	0.53±0.07 A	0.22±0.04 B	1.50±0.08 C	1.40±0.09 C	6.48±0.34 D
TN (%)	0.09±0.01 A	0.09±0.02 A	0.03±0.00 B	0.25±0.03 C	0.24±0.03 C	0.31±0.03 D
P (%)	0.07±0.00 A	0.07±0.00 A	0.07±0.00 B	0.09±0.00 C	0.08±0.00 C	0.06±0.00 B
K (%)	2.08±0.07 A	2.09±0.08 A	1.88±0.07 B	2.44±0.04 C	2.42±0.09 C	1.80±0.06 B
Mg (%)	1.39±0.06 A	1.40±0.05 A	1.22±0.08 B	1.54±0.02 C	1.53±0.04 C	1.11±0.06 B
Ca (%)	4.48±0.09 A	4.52±0.07 A	4.22±0.12 B	4.49±0.19 A	4.47±0.23 AB	4.07±0.31 B
Fe (%)	3.37±0.20 A	3.44±0.19 A	2.77±0.23 B	4.24±0.18 C	4.15±0.21 C	2.59±0.17 B
Mn (µg/g)	681.08±46.55 A	702.92±41.87 A	588.09±53.72 A	845.67±41.51 B	818.00±52.20 B	477.70±44.13 C
Zn (µg/g)	93.41±5.34 A	92.84±7.15 A	48.03±3.67 B	127.33±2.97 C	127.33±3.35 C	47.21±4.54 B
Cu (µg/g)	28.60±2.14 A	28.12±2.85 A	13.17±1.77 B	42.70±1.32 C	42.23±1.52 C	12.23±1.06 B
CIA	57.69±0.85 A	58.11±0.90 A	53.54±1.78 B	64.49±0.55 C	64.28±1.10 C	56.65±1.33 A

Different letters represent significant differences ($p < 0.05$) among types

TC: total C, SOC: soil organic C, TN: total nitrogen, CI: confidence interval (95%)

moisture content ($p < 0.05$), higher salinity ($p < 0.05$), and a higher SO₄²⁻ concentration ($p < 0.05$). The environmental conditions were different at CROWN-PA, where the soil moisture content was 65.64%. The salinity and SO₄²⁻ concentration at the CROWN-PA, which was unaffected by the tides, were the lowest. Salinities were generally in the range 10–18 PSU at the other three locations, all of which were influenced

by tides. Pore water pH was not significantly different among locations ($p > 0.05$). Locations other than CROWN-PW were classified as primary weathering sites based on their CIA values (Table 1). The CIA values as well as the concentration of Iron (Fe), Zinc (Zn), Copper (Cu) were lower at alternate control locations than the warming-experimental locations (Table 1).

Across growing seasons, warming altered plant characteristics (height and base diameter) of *Phragmites* ($p < 0.05$). However, warming increased the height of only *Spartina* significantly ($p < 0.05$), and warming caused no significant changes of base diameters across the growing season (Table 1). Warming significantly increased the AGB of *Phragmites* but not of *Spartina* (Table 2 and Table S4). Plant characteristics were of course different among locations. Plant heights were significantly higher at cCROWN-SW and cCROWN-PW compared to their corresponding alternate control location in the early growing season ($p < 0.05$). The AGB of different plant species differed significantly (Table 2). Except for September 2018, the AGB was much lower for *Spartina* than *Phragmites* (Fig. 2). Tidal restriction significantly affected the AGB of *Spartina* but did not affect *Phragmites* (Table 2). Except for the year 2018, the AGB was greater for cCROWN-SA than for cCROWN-SW throughout all seasons (Fig. 2). In contrast, during more than half of the measurement

periods, the AGB was lower for cCROWN-PA than for cCROWN-PW (Fig. 2).

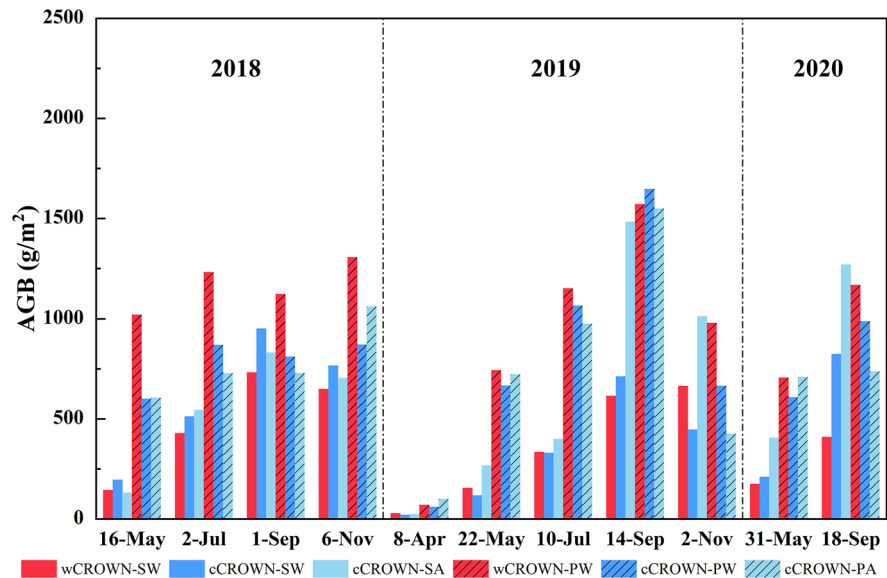
NEE, R_{eco} and CH_4 fluxes

Warming tended to inhibit the magnitude of NEE (equivalent to the absolute value of NEE). Among 8 of 11 measurement periods, the magnitude of NEE was lower at wCROWN-SW than at cCROWN-SW. Three of those differences were significant (Fig. 3a; * indicates a significant effect of warming). Warming at CROWN-PW also reduced the magnitude of NEE in 8 of 11 periods, two of which were significant (Fig. 3b; * indicated a significant effect of warming). In the early growing season, warming tended to increase R_{eco} . However, warming tended to inhibit R_{eco} in the late growing season (Fig. 3c and d; * indicated a significant effect of warming). There were no consistent effects of warming on CH_4 fluxes, but one measurement in September at peak vegetation biomass showed that warming significantly increased

Table 2 Statistical analyses for the effects of plant species, experimental warming, and tidal restriction on aboveground biomass (AGB), net ecosystem CO_2 exchange (NEE), ecosystem respiration (R_{eco}) and CH_4 fluxes for experimental studies in Yancheng, Jiangsu Province, China

Source of variation	n	f	p
AGB ($g\ m^{-2}$)			
Species (cCROWN-SA vs. cCROWN-PW)	128	5.01	<0.05
Warming (wCROWN-SW vs. cCROWN-SW)	132	1.56	0.21
Warming (wCROWN-PW vs. cCROWN-PW)	132	4.92	<0.05
Tidal (cCROWN-SW vs. cCROWN-SA)	132	5.61	<0.05
Tidal (cCROWN-PW vs. cCROWN-PA)	132	0.28	0.60
NEE ($g\ m^{-2}\ h^{-1}$)			
Species (cCROWN-SA vs. cCROWN-PW)	129	6.29	<0.05
Warming (wCROWN-SW vs. cCROWN-SW)	119	2.37	0.13
Warming (wCROWN-PW vs. cCROWN-PW)	126	0.05	0.82
Tidal (cCROWN-SW vs. cCROWN-SA)	124	0.02	0.90
Tidal (cCROWN-PW vs. cCROWN-PA)	123	15.33	<0.05
R_{eco} ($g\ m^{-2}\ h^{-1}$)			
Species (cCROWN-SA vs. cCROWN-PW)	112	7.04	<0.05
Warming (wCROWN-SW vs. cCROWN-SW)	123	0.1	0.75
Warming (wCROWN-PW vs. cCROWN-PW)	110	0.14	0.71
Tidal (cCROWN-SW vs. cCROWN-SA)	126	0.41	0.53
Tidal (cCROWN-PW vs. cCROWN-PA)	121	0.82	0.37
CH_4 ($mg\ m^{-2}\ h^{-1}$)			
Species (cCROWN-SA vs. cCROWN-PW)	126	8.04	<0.05
Warming (wCROWN-SW vs. cCROWN-SW)	126	0.03	0.87
Warming (wCROWN-PW vs. cCROWN-PW)	119	0.18	0.68
Tidal (cCROWN-SW vs. cCROWN-SA)	128	18.57	<0.05
Tidal (cCROWN-PW vs. cCROWN-PA)	125	18.09	<0.05

Fig. 2 Seasonal variation of *Phragmites australis* and *Spartina alterniflora* aboveground biomass (AGB) by treatment and growing season for experimental studies in Yancheng, Jiangsu Province, China



CH₄ fluxes in CROWN-PW (Table 2; Fig. 3e; * indicated a significant effect of warming). However, the responses of NEE, R_{eco} , and CH₄ flux to warming were not significant if all the measured fluxes were included in the analyses (Table 2).

The NEE, R_{eco} , and CH₄ flux varied significantly between plant species ($p < 0.05$, Table 2). The R_{eco} and CH₄ flux of cCROWN-SA were significantly higher than those of cCROWN-PW (Table 2, Table S4 and Fig. 3). However, the magnitude of NEE was higher in *Phragmites* wetlands (Table 2, Table S4 and Fig. 3). GHG exchange showed clear seasonal patterns, except for CH₄ fluxes in CROWN-PA (Fig. 3).

Among 10 of 11 measurement periods, the magnitude of NEE was lower at cCROWN-PA than at cCROWN-PW (Fig. 3b), especially in the middle of the 2019 growing season. Remarkably, the CH₄ fluxes were greater at both alternate control locations (CROWN-SA and CROWN-PA) and those CH₄ fluxes was significant higher ($p < 0.05$) than the corresponding fluxes at the warming-experimental locations (CROWN-SW and CROWN-PW) throughout all seasons and years (Fig. 3e and f).

NEE, R_{eco} and CH₄ fluxes versus environmental parameters and plant characteristics

Net ecosystem CO₂ exchange (NEE) peaked at 25 °C in the *Phragmites* wetland, but NEE did not

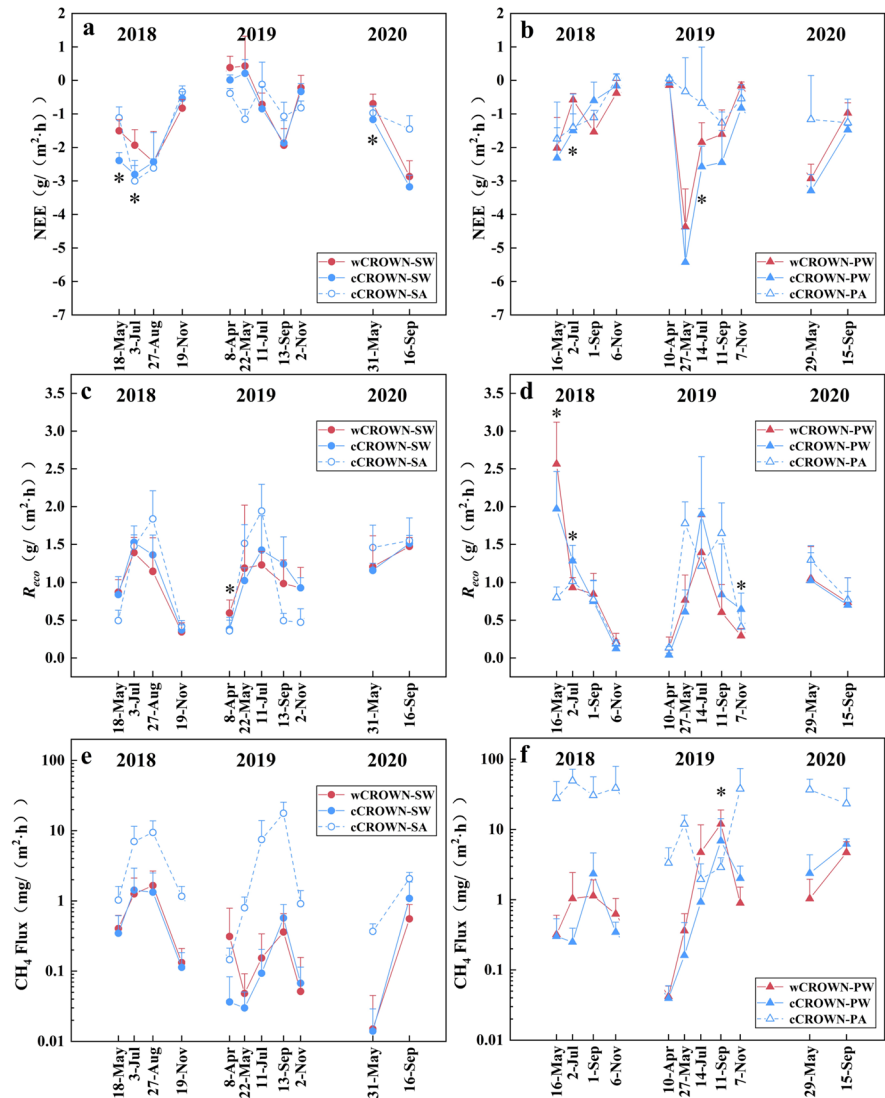
peak until 35 °C in the *Spartina* wetland (Figs. 4a and 5). The NEE was inversely related to WTD, salinity and AGB ($p < 0.018$, Table 3). The NEE in both vegetation types peaked at a salinity of ~15 PSU (Fig. 4b). There was a direct relationship between R_{eco} and air temperature ($p < 0.01$, Table 3; Fig. 4d). The temperature effects on CH₄ fluxes were a little less straightforward. Generally, high values of CH₄ fluxes corresponded to temperatures higher than ~18 °C. However, in the freshwater CROWN-PA, CH₄ fluxes did not follow this pattern, and high values were found at temperatures below 18 °C (Fig. 4g). Methane fluxes tended to be negligible at air temperature lower than 18 °C if measurements were made at salinities more than 5 PSU (Fig. 4h). Methane flux was negatively related to salinity ($p < 0.018$, Table 3), and were extremely high when the WTD was above the soil surface (Fig. 4i).

Annual greenhouse gas flux and radiative balance

Annual GHG fluxes were estimated by integration of smooth curves fit to the daily fluxes. The methodology is illustrated in Fig. 6 in the case of the R_{eco} data at cCROWN-SW and cCROWN-PW. The red cross in Fig. 6b is the point that was ignored because it was outside the 95% prediction bands.

Table 4 shows the annual greenhouse gas (GHG) flux estimates and radiative balance calculations from

Fig. 3 Seasonal variation in NEE, R_{eco} , and CH_4 fluxes for experimental studies in Yancheng, Jiangsu Province, China (* indicates the response of GHG fluxes to warming is significant, $p < 0.05$)



our experimental studies. Because the responses of the GHG exchange fluxes to warming were significant during some monitoring periods (Fig. 3), we estimated the annual GHG fluxes for the warming types (wCROWN-SW and wCROWN-PW). We believe that the warming effect would be very apparent if it were integrated throughout the year.

On the one hand, warming decreased the magnitude of annual NEE by 19% for the CROWN-SW and decreased the magnitude of annual NEE by 11% for the CROWN-PW. On the other hand, warming increased the annual CH_4 fluxes by 28% for the CROWN-PW and generated no significant changes for the CROWN-SW. Moreover, warming had little

influence on the annual R_{eco} fluxes (Table 4). Warming increased the radiative balance (in $kg\ CO_2\text{-eq}/(m^2\cdot yr)$) of the ecosystem from -4.16 to -0.74 to -3.32 to 0.02 for CROWN-SW, and from -4.97 to -2.82 to -4.13 to -2.05 for CROWN-PW. The magnitude of the annual NEE of cCROWN-SA was significantly lower than that of cCROWN-PW. However, cCROWN-SA had a higher annual R_{eco} and annual CH_4 flux than cCROWN-PW. A significant finding was that the annual CH_4 flux was particularly high ($218.72\ g/(m^2\cdot yr)$) in the freshwater *Phragmites* wetland at cCROWN-PA, where it was ~ 58 times the lowest value measured at other types, a highly improbable result by random chance

Table 3 Results of experimental studies in Yancheng, Jiangsu Province, China from linear mixed-effects models, with NEE, Reco, and CH₄ fluxes as response variables

Response variable	Predictor	Coefficient	SE	<i>p</i>
NEE	WTD	-210.4602	201.7206	<i>n</i> = 305 < 0.001
	Salinity	-126.1142	14.2579	< 0.001
	AGB	-0.4422	0.1859	0.018
<i>R</i> _{eco}	Air temperature	40.3440	6.8145	<i>n</i> = 287 < 0.001
				<i>n</i> = 310
CH ₄	Salinity	-0.8916	0.3755	0.018

The fixed factors were air temperature, WTD, salinity, and AGB

Coefficients were included in Eq. (7), SE was standard deviation of mean value

NEE: net ecosystem CO₂ exchange, *R*_{eco}: ecosystem respiration, WTD: water table depth, AGB: aboveground biomass

(Table 4). Moreover, the magnitude of annual NEE at CROWN-PA was also the lowest. The range of radiative balance at CROWN-PA was 7.11 to 9.64 kg CO₂-eq/(m²·yr). The next highest annual CH₄ flux was 33.52 g/(m²·yr) at CROWN-SA, which was ~9 times the lowest value measured at other locations. The range of radiative balance at CROWN-SA thus reached -2.61 to 0.67 kg CO₂-eq/(m²·yr).

Discussion

Responses of NEE, *R*_{eco} and CH₄ fluxes to warming

Our study area is in a subtropical zone where temperatures are high during the entire growing season. The highest daily average temperature reaching 30 °C. The additional warming that made the air temperature far exceed the optimum temperature for *Spartina* (30 °C) and *Phragmites* (25 °C) likely reduced the photosynthetic performance (Ge et al. 2014) and resulted in a reduction of the magnitude of NEE (Fig. 3a and b, * indicates a significant effect of warming). The cooling effect of plant transpiration was weakened because of the reduction in the air circulation within the OTC, and the resultant extremely high temperature of leaf surfaces further exacerbated the stress (Thongbai et al. 2010). Our previous study

of leaf-scale photosynthetic performance (Jiang et al. 2022) also confirmed that warming does inhibit the photosynthetic performance of *Phragmites*. *Spartina*, as a C4 plant, has greater ability to acclimate to temperature. However, the main reason for the reduction of the magnitude of the NEE of *Spartina* by warming in this study (Fig. 3a) was likely the significantly higher salinity and lower WTD in the warming plots (Table 1) due to warming-enhanced evaporation. Overall, the response of NEE to this extent of warming was not significant (Table 2). Some studies have found that similar proportionate increases of Reco and GPP due to warming result in no significant change of NEEs (Chivers et al. 2009; Oberbauer et al. 2007). Other studies suggest that OTC failed to provide long-term effective warming to alter NEE, which may be related to the high humidity environment, where heat was lost in the form of latent heat (Johnson et al. 2013; Pearson et al. 2015). In addition, the response results of GHG exchange to warming is essentially a cumulative effect of the ecosystem over the entire experimental period (Oberbauer et al. 2007). In other words, the results now may depend on early responses from experiments a few years ago. And results in the middle and late growing seasons within a year may also depend on responses in the earlier growing season. This temporal asymmetry may also weaken the strength of the NEE-warming relationship.

The response of *R*_{eco} to warming depended on the period of growing season (Fig. 3). Previous studies have shown that warming stimulates the activities of plants and microbes (Chivers et al. 2009; Fouche et al. 2014) and accelerated plant growth and microbial reproduction. Enhancement of biological respiration and soil organic matter decomposition will lead to an increase of *R*_{eco}. This mechanism may account for the significant increase of *R*_{eco} in the early growing season at CROWN-SW and CROWN-PW (Fig. 3c and d; * indicated a significant effect of warming). Unlike most previous warming studies that have focused on high latitudes, our study area was located in the subtropics, where the average annual temperature is higher and the plant growing season longer than at higher latitudes. A reversal in the response of *R*_{eco} to warming was occurred in the late growing season, as there were a few cases of significant lower fluxes of *R*_{eco} within warming plots, presumably due to warming stress (Fig. 3c and d; * indicated a significant

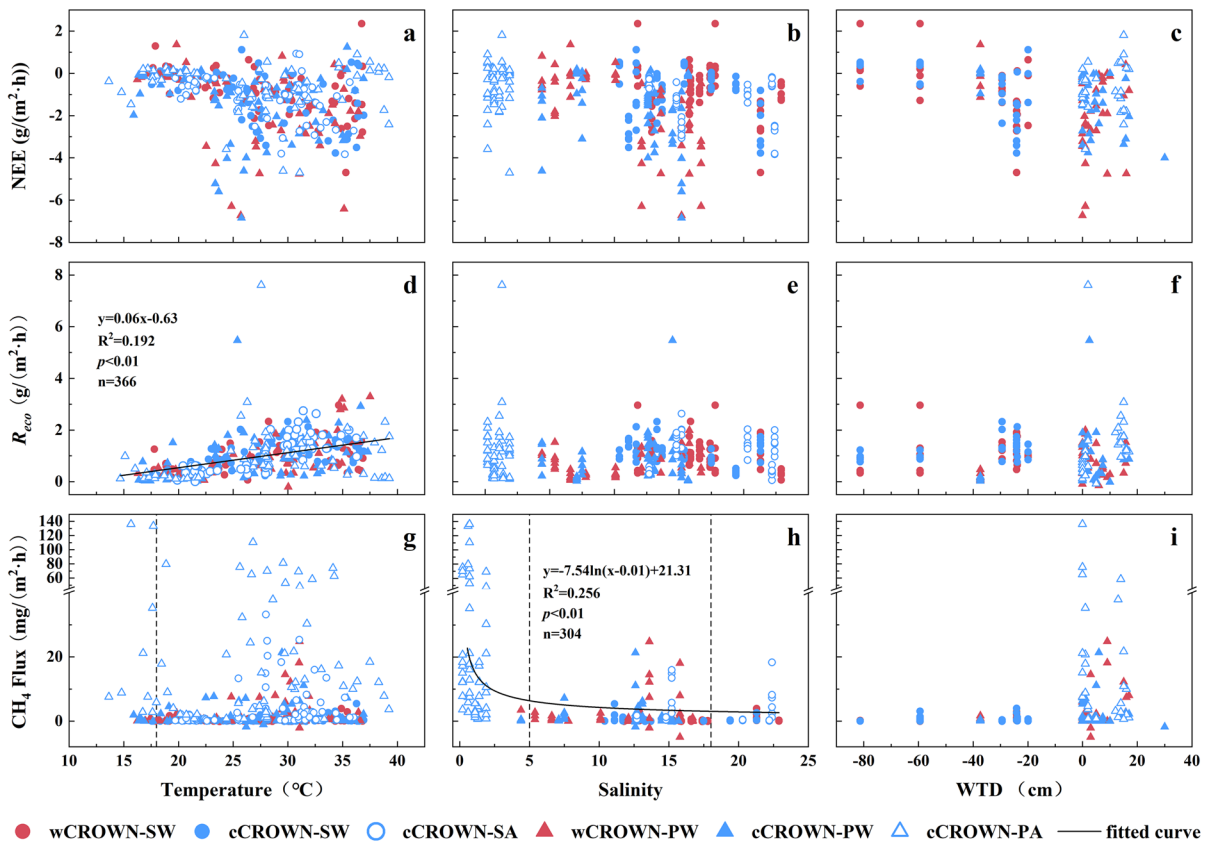


Fig. 4 Air temperature, salinity and water table depth versus NEE, R_{eco} and CH_4 fluxes for experimental studies in Yancheng, Jiangsu Province, China. (Positive water table depth

values indicate that the water table was above the soil surface (flooded), while negative values indicate that the water table was below the soil surface)

Fig. 5 Relationships between NEE and temperature in CROWN-S (a) and between NEE and temperature in CROWN-P (b) for experimental studies in Yancheng, Jiangsu Province, China. Runs tests were based on sequences of values above or below the horizontal lines (the average values)

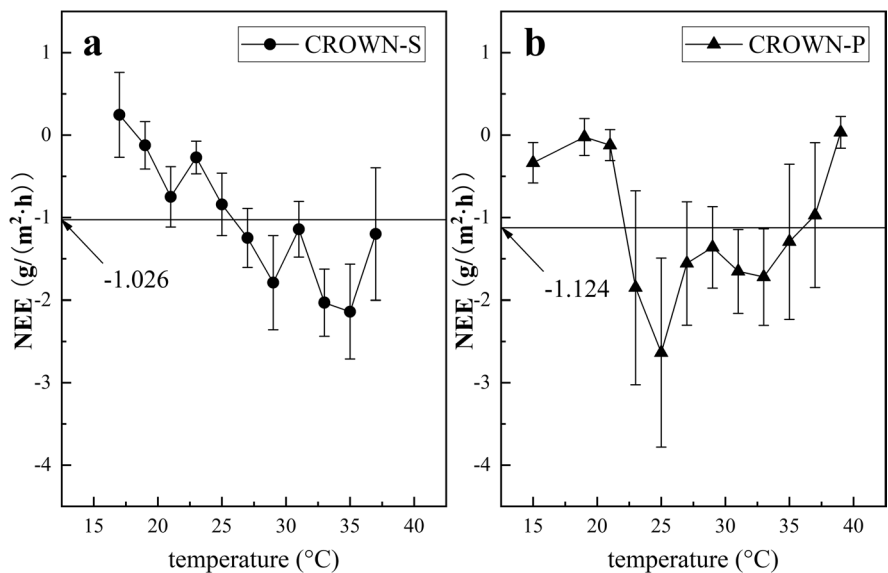


Fig. 6 Daily R_{eco} fluxes versus day of year for data collected at the cCROWN-SW and cCROWN-PW, respectively. The red cross indicates a datum that was ignored because it was outside the 95% prediction bands. The annual flux was estimated by integration of the area under the smooth curve

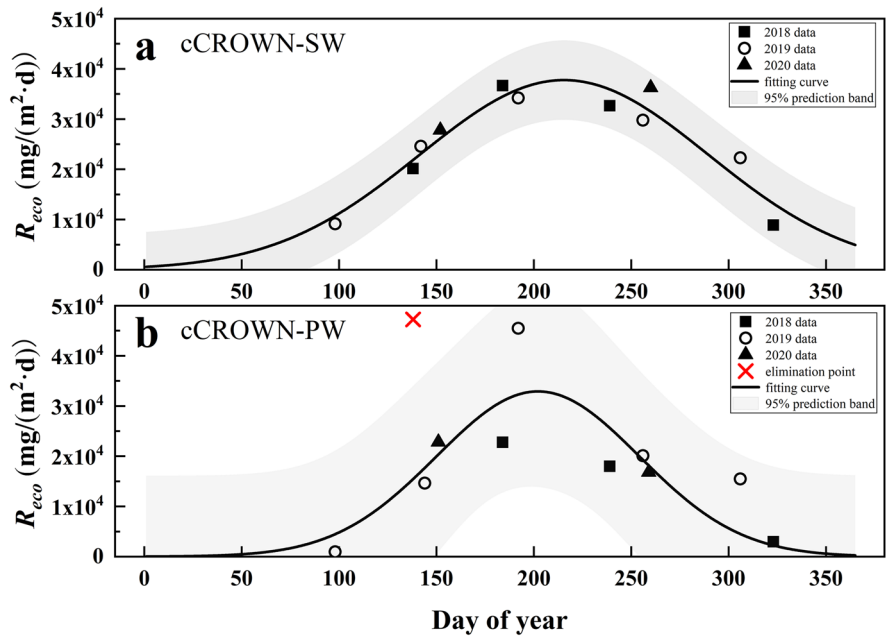


Table 4 Annual greenhouse gas (GHG) flux and radiative balance range for experimental studies in Yancheng, Jiangsu Province, China

Types	Annual GHG flux kg/ (m ² ·yr)			CO ₂ -equivalent GHG flux kg CO ₂ -eq/ (m ² ·yr)			Radiation balance range kg CO ₂ -eq/ (m ² ·yr)	Carbon source and sink judgment
	NEE	R_{eco}	CH ₄	NEE (SGCP)	R_{eco} (night) (SGWP)	CH ₄ (SGWP)		
wCROWN-SW	-3.49	6.89	3.77×10^{-3}	-3.49	3.34	0.17	-3.32 to 0.02	sink or weak source
cCROWN-SW	-4.33	6.84	3.77×10^{-3}	-4.33	3.42	0.17	-4.16 to -0.74	sink
cCROWN-SA	-4.11	6.56	33.52×10^{-3}	-4.11	3.28	1.51	-2.61 to 0.67	sink or weak source
wCROWN-PW	-5.05	4.17	20.41×10^{-3}	-5.05	2.09	0.92	-4.13 to -2.05	sink
cCROWN-PW	-5.68	4.30	15.88×10^{-3}	-5.68	2.15	0.71	-4.97 to -2.82	sink
cCROWN-PA	-2.73	5.06	218.72×10^{-3}	-2.73	2.53	9.84	7.11 to 9.64	source

The calculation of the lowest value and the highest value of the radiation balance range assumes that the R_{eco} at night is 0, and the R_{eco} is the same at night and during the daytime, respectively

SGWP: sustain-flux global warming potential; SGCP: sustain-flux global cooling potential. NEE: net ecosystem CO₂ exchange, R_{eco} : ecosystem respiration

effect of warming). Although R_{eco} was highly correlated with variations of air temperature ($p < 0.001$, Table 3), the response of R_{eco} to this magnitude of warming was not significant ($p > 0.05$, Table 2). From the perspective of temperature sensitivity (Q_{10}) of R_{eco} , even assuming that the Q_{10} is as large as 3 (Mahecha et al. 2010), the increases of R_{eco} caused by warming were within the range of the noise of the data (Appendix S1: Section S1).

The response of CH₄ fluxes to warming was insignificant (Table 2) with the exception of one measurement made on 11 September in the CROWN-PW. Previous studies have shown that CH₄ fluxes do not respond significantly to OTC-induced warming, but rather to changes in WTD (Li et al. 2021; Munir and Strack 2014; Pearson et al. 2015). In other words, temperature is not the dominant factor affecting CH₄ flux relative to the hydrological factors that control

redox conditions. Moreover, the changes of the soil temperature of the OTC in our study were apparently not consistent and positive enough to stimulate changes in microbial mineralization and decomposition (Appendix S1: Figs. S2 and S3). A previous active warming experiment showed that the response of CH₄ flux to warming was significantly increased by an increase of soil temperature greater than 5 °C (Hopple et al. 2020; Noyce and Megonigal 2021). Our study also showed that if the magnitude of the temperature change was large enough (from 25 to 30 °C), the response of the CH₄ flux to the temperature increase was obvious (Fig. 4g, excluding data from the cCROWN-PA). In addition, there may be lag in the response of CH₄ flux to warming, and top-down warming (OTC-induced) presumably prolong this lag period (Hopple et al. 2020).

Responses of NEE, R_{eco} and CH₄ fluxes to plant species

The significant difference in NEE between native *Phragmites* and invasive *Spartina* was mainly due to the difference in AGB (Table 2). The significant increase of photosynthetic leaf area with an increase of AGB and vegetation cover (Guo et al. 2021), explains the negative correlation between NEE and AGB ($p=0.018$, Table 3). The advantage of *Phragmites* in AGB was particularly manifested in plant height (Table 1), which undoubtedly contributes to its capacity to absorb solar energy and CO₂. The fact that the temperature at which the peak of NEE appeared was lower at CROWN-P than at CROWN-S indicated that the optimum temperature for photosynthesis was lower for *Phragmites* than for *Spartina* (Figs. 4a and 5). However, it cannot be concluded that *Spartina* sequesters more carbon than *Phragmites* as the climate warms. When the temperature exceeded 25 °C, the magnitude of NEE decreased at CROWN-P, but it was still not lower than that at CROWN-S. The effect of changes in WTD and salinity on NEE should be attributed to tidal restriction rather than plant species.

The fact that R_{eco} was higher in invasive *Spartina* than in native *Phragmites* ($p<0.05$, Table 2 and Table S4), was consistent with previous studies (Liao et al. 2007; Zhang et al. 2010b; Zhou et al. 2015). *Spartina* may affect R_{eco} by altering the quantity and quality of input organic matter (Inglett et al. 2012; Xu et al. 2014). However, in our study, the AGB and

SOC of CROWN-SA were significantly lower than those of CROWN-PW (Table 1; Fig. 2). And high R_{eco} also occurred in CROWN-SW, which was less affected by tides (Fig. 3c). The results revealed that the reduction of AGB and changes in the redox conditions of the environment did not limit the occurrence of high R_{eco} in the *Spartina*. There were hence other factors that may have stimulated the increase of R_{eco} . We hypothesized that there were two reasons: first, the respiration rate of *Spartina*, a C4 plant, is higher than that of *Phragmites*, a C3 plant (Xu et al. 2014); Second, *Spartina* may transport more photosynthate underground than *Phragmites* to provide substrates for respiration (Chen et al. 2016).

In CROWN-SW, the CH₄ fluxes were significantly lower in invasive *Spartina* than native *Phragmites* (Fig. 3). Compared with *Phragmites*, *Spartina* has a more well-developed root system, higher root density, and finer taproots. These characteristics facilitate the accumulation of oxygen in the rhizosphere for CH₄ oxidation (Xu et al. 2014). In situ studies showed that *Spartina* oxidizes CH₄ more rapidly, presumably because of its well-developed aerenchyma and gas transport capacity (Tong et al. 2012). However, we suggest that the low CH₄ fluxes at CROWN-SW should be attributed to water deficit caused by tidal restriction rather than to differences of plant species. The CH₄ fluxes of CROWN-PW were no greater or even lower than those of CROWN-SA, which was more strongly affected by tides and had a higher WTD (Table 1; Fig. 3). Yuan et al. (2015) also found that CH₄ release from *Spartina* was higher than that from *Phragmites* because of its location in a more saturated soil environment. In other words, if sea level continues to rise, the CH₄ fluxes of CROWN-SW will presumably increase substantially and even surpass those of *Phragmites*. This pattern has been observed in other experimental mesocosm studies (Cheng et al. 2007; Zhang et al. 2010a). The CH₄ fluxes from CROWN-SA may therefore be indicative of the CH₄ fluxes from CROWN-SW in the future.

Responses of NEE, R_{eco} and CH₄ fluxes to tidal restriction

Human activities, such as road building, damming, and crab trapping (via crab trapping trench and fences), could restrict the tidal exchange between the warming-experimental locations

and the alternate control locations. Tidal restriction commonly causes differences of salinity and WTD that affect GHG exchanges in salt marsh wetlands (Portnoy 1999).

Several studies have found that increased salt stress can inhibit the magnitude of NEE in coastal wetland ecosystems, especially during the early growing season (Abdul-Aziz et al. 2018; Volik et al. 2020; Wei et al. 2020). Increasing salinity adversely affects lipid metabolism and the synthesis of chlorophyll and protein in leaves. The resultant reduction of the photosynthetic rates of plants will adversely affect plant growth and the magnitude of NEE (Parida and Das 2005; Pierfelice et al. 2017). However, in our study, elevated salinity enhanced the magnitude of NEE at CROWN-PW compared to CROWN-PA (Fig. 4b). The explanation may be a moderate increase of salinity has little effect on the chlorophyll content and photosynthetic parameters of *Phragmites* but improves its water use efficiency (Li et al. 2018; Pagter et al. 2009). For example, Gorai et al. (2010) found that *Phragmites* grows best in a low-oxygen, moderate-salt environment. We hypothesize that *Phragmites* may produce additional low-molecular-weight compounds via more rapid photosynthesis to acclimate the ion balance within the plant and assimilate more C in this process (Parida and Das 2005). WTD is the basic condition for controlling NEE ($p < 0.001$, Table 3). Due to tidal restriction, the WTD was significantly lower for CROWN-SW than for CROWN-SA. That difference in WTD may explain the positive NEE at CROWN-SW (Fig. 3). Water deficit can be a threat to wetland plants, and the role of wetlands as C sinks can be constrained. For example, water willow in the southeastern United States experienced limited growth, productivity, and survival after more than two weeks of drought (Touchette and Steudler 2009). Chu et al. (2019) have also highlighted the fact that a high soil moisture content promotes plant biomass and the magnitude of NEE early in the growing season. Unlike CROWN-PW (the WTD was below the soil surface at low tide), which is affected by tides, tidal restriction caused a persistent retention of freshwater at the CROWN-PA. The CIA of CROWN-PA was lower because of long-term anaerobic conditions at that location (Table 1). The reduced production via weathering of Fe, Zn, Cu, essential trace elements for plant growth (Kaur et al. 2022; Lehmann et al. 2014), may have reduced the magnitude of NEE.

In our study, the weak responsiveness to variations of salinity exhibited by R_{eco} (Fig. 4e) was contrary to the findings of previous studies (Huang et al. 2020; Wei et al. 2020). Generally, salinity stress reduces microbial cell activity and adversely affects plant growth (Chambers et al. 2016; Li et al. 2018). However, in coastal wetland ecosystems, different plants acclimate to different salinity gradients, and the same plants can also acclimate to different salinity gradients because of their high plasticity and/or genetic factors (Brix 1999; Clevering and Lissner 1999). The fact that salinity gradient have not caused variations of microbial respiration (Yan and Marschner 2013) may explain why R_{eco} responded weakly to salinity variations. In the case of flooding, both autotrophic and heterotrophic respiration would be inhibited (Chivers et al. 2009), and the diffusion of CO_2 could be hindered and some of the CO_2 captured by water (Han et al. 2015). The fact that the vascular structure of wetland plants helps alleviate the impact of flood stress on R_{eco} (Brix et al. 2001) explains why the R_{eco} exhibited no consistent pattern in response to WTD (Fig. 4f). Overall, R_{eco} was not affected by tidal restriction because of the ability of plants and microbes in coastal wetlands to acclimate to different salinity gradients and flooding conditions.

Water table depth (WTD) is an important determinant of soil redox conditions, which are an important determinant of CH_4 fluxes (Zhao et al. 2020). Tidal restriction exposed the soil to oxygen and resulted in a lower flux of CH_4 at CROWN-SW (Fig. 4i). When the WTD rose to the soil surface, it was no longer a limiting condition for CH_4 release, and the fluxes depended on salinity, temperature, or other environmental factors. Our result also showed a significant relationship between CH_4 flux and salinity ($p = 0.018$, Table 3). Consistent with most previous studies, increased salinity suppressed CH_4 production, mainly because sulfate reduction took precedence over methanogenesis (Capooci et al. 2019; Olsson et al. 2015; Poffenbarger et al. 2011). Tidal restriction lowers the salinity in landward wetlands (Emery and Fulweiler 2017) and therefore led to significant CH_4 production at CROWN-PA (Fig. 4h). Under unique environmental conditions, the flux of CH_4 can be high even at low temperatures. Strong evidence of this was the extremely high CH_4 fluxes at temperatures below 18 °C at CROWN-PA (Fig. 4g), where there were high concentrations of organic C and nutrients in the

soil, an elevated WTD, and low salinity (Table 1). There were hence sufficient available substrates for CH₄ generation, good reduction conditions, and weak competition from sulfate reduction. It should be noted that the changes in salinity and SO₄²⁻ concentration do not necessarily occur synchronously. Compared with CROWN-SW, CROWN-SA has higher salinity and lower SO₄²⁻ concentration (Table 1). We infer that the SO₄²⁻ concentration decreased due to partial reduction to H₂S under better reducing conditions. This may be another reason for the higher CH₄ flux in CROWN-SA.

Carbon source and sink judgment

Warming weakened the magnitude of the annual NEE and resulted in a more positive radiation balance at the two warming types. The wCROWN-SW possibly became a weak carbon source (−3.32 to 0.02 kg CO₂-eq m⁻² yr⁻¹). Compared with the *Phragmites* in CROWN-PW, *Spartina* in CROWN-SA decreased the annual NEE and increased the annual R_{eco} and CH₄ flux. *Spartina* overall reduces the carbon sink capacity of coastal salt marshes, and this effect is further exacerbated by tidal restoration or future sea level rise. Although CROWN-SA and CROWN-SW were carbon sinks, both were occasionally weak carbon sources (i.e. positive radiation balances). Tidal restriction severely affected the radiative balance of the *Phragmites* wetland from a consistent carbon sink (−4.97 to −2.82 kg CO₂-eq m⁻² yr⁻¹) to a consistent carbon source (7.11 to 9.64 kg CO₂-eq m⁻² yr⁻¹) by decreasing the magnitude of the annual NEE and increasing the annual CH₄ flux.

In summary, tidal restriction may have a greater impact on the carbon sinks of coastal wetlands than climate warming and invasive plants. Tidal restriction in the form of dams and roads directly affected wetland WTD and salinity. Carbon uptake by plants and anaerobic decomposition of organic matter were thus affected. The result has been a decrease of carbon storage potential and extreme changes in CH₄ emissions in the coastal wetlands studied.

Climate warming and plant species may also affect the carbon cycle of coastal wetlands, but the impact may be limited. The wCROWN-SW and cCROWN-SA were weak carbon sources because of warming and changes in plant species. However, the positive radiative balance occurred near the boundary

condition (assuming that R_{eco} was the same during the night and daytime). This result and the high positive correlation between R_{eco} and temperature ($p < 0.01$) suggest that these C sources may be overestimates. In other words, if the future climate warming is controlled below 1.5 °C and the scale of *Spartina* invasion remains the same, climate warming and plant species may have less impact on the carbon sink function of coastal wetlands. Further studied could help improve understanding of the impact of tidal restriction on the carbon sink of coastal wetlands. We acknowledge that the annual flux of GHG exchange may be overestimated by the chamber method. But our objective in estimating annual flux was to examine the mechanisms by which warming, plant species and tidal restriction affect GHG exchange in coastal wetlands, rather than to obtain precise values of annual flux for carbon trading purposes.

Concluding remarks

If the future temperature increase can be controlled within 1.5 °C, the magnitude of the radiative balance of native *Phragmites* might be reduced, but the direction is unlikely to change, and *Phragmites* will remain a consistent carbon sink. However, there is a risk of invasive *Spartina* becoming a carbon source under the influence of climate warming or sea level rise due to lower in AGB and the magnitude of NEE and higher in R_{eco} and CH₄ flux compared with native *Phragmites*. Notably, freshwater *Phragmites* wetlands formed by tidal restriction reduced the magnitude of NEE and substantially increased CH₄ emissions. the result was a consistent carbon source.

Acknowledgements This research was jointly funded by Laoshan Laboratory (LSKJ2022040003), the National Natural Science Foundation of China (No. U22A20558), the Natural Science Foundation of Shandong Province (ZR2023MD060), the National Key R&D Program of China (2016YFE0109600), the Foundation of the Yellow Sea Wetland Research Institute (20210108), and the China Geological Survey Program (DD20221775 & DD20189503). We would like to express our gratitude to the two reviewers for their constructive comments on the revisions. Any use of trade, firm, or product names is for descriptive purposes only and does not imply endorsement by the U.S. Government.

Author contributions Conceptualisation: Siyuan Ye, Ken W Krauss, Samantha K. Chapman, Shucheng Xie; Methodology:

Siyuan Ye, Ken W Krauss, Pan Zhou, Liujuan Xie, Lixin Pei; Investigation: Pan Zhou, Liujuan Xie, Lixin Pei, Hongming Yuan, Shixiong Yang, Xigui Ding; Resources: Siyuan Ye; Formal Analysis: Pan Zhou, Siyuan Ye, Edward A. Laws; Writing – Original Draft Preparation: Pan Zhou; Writing – Review & Editing: all.

Funding This research was jointly funded by Laoshan Laboratory (LSKJ2022040003), the National Natural Science Foundation of China (No. U22A20558), the Natural Science Foundation of Shandong Province (ZR2023MD060), the National Key R&D Program of China (2016YFE0109600), the Foundation of the Yellow Sea Wetland Research Institute (20210108), and the China Geological Survey Program (DD20221775 & DD20189503).

Data availability The data generated and/or analyzed during the current study are available from the corresponding author on reasonable request.

Declarations

Competing interests The authors have no relevant financial or non-financial interests to disclose.

References

- Abdul-Aziz O, Ishiaq K, Tang J, Moseman-Valtierra S, Kroeger K, Gonnee M, Mora J, Morkeski K (2018) Environmental controls, emergent scaling, and predictions of greenhouse gas (GHG) fluxes in coastal salt marshes. *J Geophys Res: Biogeosci* 123:2234–2256. <https://doi.org/10.1029/2018JG004556>
- Angst G, Mueller KE, Kögel-Knabner I, Freeman KH, Mueller CW (2017) Aggregation controls the stability of lignin and lipids in clay-sized particulate and mineral associated organic matter. *Biogeochemistry* 132:307–324. <https://doi.org/10.1007/s10533-017-0304-2>
- Barthol J, Dignac MF, Le Mer G, Bottinelli N, Wateau F, Kögel-Knabner I, Rumpel C (2020) How do earthworms affect organic matter decomposition in the presence of clay-sized minerals? *Soil Biol Biochem* 143:107730. <https://doi.org/10.1016/j.soilbio.2020.107730>
- Bottollier-Curtet M, Planty-Tabacchi A-M, Tabacchi E (2013) Competition between young exotic invasive and native dominant plant species: implications for invasions within riparian areas. *J Veg Sci* 24:1033–1042. <https://doi.org/10.1111/jvs.12034>
- Bradley BA, Houghton RA, Mustard JF, Hamburg SP (2006) Invasive grass reduces aboveground carbon stocks in shrublands of the western US. *Glob Change Biol* 12:1815–1822. <https://doi.org/10.1111/j.1365-2486.2006.01232.x>
- Brix H (1999) Genetic diversity, ecophysiology and growth dynamics of reed (*Phragmites australis*). *Aquat Bot* 64:179–184
- Brix H, Sorrell BK, Lorenzen B (2001) Are *Phragmites*-dominated wetlands a net source or net sink of greenhouse gases? *Aquat Bot* 69:313–324. [https://doi.org/10.1016/S0304-3770\(01\)00145-0](https://doi.org/10.1016/S0304-3770(01)00145-0)
- Capooci M, Barba J, Seyfferth AL, Vargas R (2019) Experimental influence of storm-surge salinity on soil greenhouse gas emissions from a tidal salt marsh. *Sci Total Environ* 686:1164–1172. <https://doi.org/10.1016/j.scitotenv.2019.06.032>
- Chambers LG, Guevara R, Boyer JN, Troxler TG, Davis SE (2016) Effects of Salinity and Inundation on Microbial Community structure and function in a Mangrove Peat Soil. *Wetlands* 36:361–371. <https://doi.org/10.1007/s13157-016-0745-8>
- Chapman SK, Feller IC, Canas G, Hayes MA, Dix N, Hester M, Morris J, Langley JA (2021) Mangrove growth response to experimental warming is greatest near the range limit in northeast Florida. *Ecology* 102. <https://doi.org/10.1002/ecy.3320>
- Chapman SK, Hayes MA, Kelly B, Langley JA (2019) Exploring the oxygen sensitivity of wetland soil carbon mineralization. *Biol Lett* 15:20180407. <https://doi.org/10.1098/rsbl.2018.0407>
- Chen YP, Chen GC, Ye Y (2015) Coastal vegetation invasion increases greenhouse gas emission from wetland soils but also increases soil carbon accumulation. *Sci Total Environ* 526:19–28. <https://doi.org/10.1016/j.scitotenv.2015.04.077>
- Chen J, Wang Q, Li M, Liu F, Li W (2016) Does the different photosynthetic pathway of plants affect soil respiration in a subtropical wetland? *Ecol Evol* 6:8010–8017. <https://doi.org/10.1002/ece3.2523>
- Cheng X, Peng R, Chen J, Luo Y, Zhang Q, An S, Chen J, Li B (2007) CH₄ and N₂O emissions from *Spartina alterniflora* and *Phragmites australis* in experimental mesocosms. *Chemosphere* 68:420–427. <https://doi.org/10.1016/j.chemosphere.2007.01.004>
- Chivers MR, Turetsky MR, Waddington JM, Harden JW, McGuire AD (2009) Effects of Experimental Water table and temperature manipulations on Ecosystem CO₂ fluxes in an alaskan Rich Fen. *Ecosystems* 12:1329–1342. <https://doi.org/10.1007/s10021-009-9292-y>
- Chmura GL, Anisfeld SC, Cahoon DR, Lynch JC (2003) Global carbon sequestration in tidal, saline wetland soils. *Glob Biogeochem Cycles* 17:n/a. <https://doi.org/10.1029/2002gb001917>
- Chu X, Han G, Xing Q, Xia J, Sun B, Li X, Yu J, Li D, Song W (2019) Changes in plant biomass induced by soil moisture variability drive interannual variation in the net ecosystem CO₂ exchange over a reclaimed coastal wetland. *Agric For Meteorol* 264:138–148. <https://doi.org/10.1016/j.agrfor.2018.09.013>
- Clevering OA, Lissner J (1999) Taxonomy, chromosome numbers, clonal diversity and population dynamics of *Phragmites australis*. *Aquat Bot* 64:185–208. [https://doi.org/10.1016/S0304-3770\(99\)00059-5](https://doi.org/10.1016/S0304-3770(99)00059-5)
- Davidson IC, Cott GM, Devaney JL, Simkanin C (2018) Differential effects of biological invasions on coastal blue carbon: a global review and meta-analysis. *Glob Change Biol* 24:5218–5230. <https://doi.org/10.1111/gcb.14426>

- Ding XR, Kang YY, Mao ZB, Sun YL, Li S, Gao X, Zhao XX (2014) Analysis of largest tidal range in rdial sand ridges southern Yellow Sea. *Acta Oceanol Sinica*(in Chinese) 36:12–20
- Ding XG, Ye SY, Laws EA, Mozdzer TJ, Yuan HM, Zhao GM, Yang SX, He L, Wang J (2019) The concentration distribution and pollution assessment of heavy metals in surface sediments of the Bohai Bay, China. *Mar Pollut Bull* 149:110497. <https://doi.org/10.1016/j.marpolbul.2019.110497>
- Drexler JZ, Krauss KW, Sasser MC, Fuller CC, Swarzenski CM, Powell A, Swanson KM, Orlando J (2013) A long-term comparison of carbon sequestration rates in impounded and naturally tidal freshwater marshes along the lower Waccamaw river, South Carolina. *Wetlands* 33:965–974. <https://doi.org/10.1007/s13157-013-0456-3>
- Duarte CM, Losada IJ, Hendriks IE, Mazarrasa I, Marbà N (2013) The role of coastal plant communities for climate change mitigation and adaptation. *Nat Clim Change* 3:961–968. <https://doi.org/10.1038/nclimate1970>
- Duarte CM, Middelburg JJ, Caraco N (2005) Major role of marine vegetation on the oceanic carbon cycle. *Biogeochemistry* 2:1–8. <https://doi.org/10.5194/bg-2-1-2005>
- Emery HE, Fulweiler RW (2017) Incomplete tidal restoration may lead to persistent high CH₄ emission. *Ecosphere* 8:e01968. <https://doi.org/10.1002/ecs2.1968>
- Fouche J, Keller C, Allard M, Ambrosi JP (2014) Increased CO₂ fluxes under warming tests and soil solution chemistry in Histic and Turbic Cryosols, Salluit, Nunavik Can Soil Biol Biochem 68:185–199. <https://doi.org/10.1016/j.soilbio.2013.10.007>
- Ge ZM, Guo HQ, Zhao B, Zhang LQ (2015) Plant invasion impacts on the gross and net primary production of the salt marsh on eastern coast of China: insights from leaf to ecosystem. *J Geophys Res-Biogeosci* 120:169–186. <https://doi.org/10.1002/2014jg002736>
- Ge ZM, Zhang LQ, Yuan L, Zhang C (2014) Effects of salinity on temperature-dependent photosynthetic parameters of a native C3 and a non-native C4 marsh grass in the Yangtze Estuary, China. *Photosynthetica* 52:484–492. <https://doi.org/10.1007/s11099-014-0055-4>
- Gorai M, Ennajeh M, Khemira H, Neffati M (2010) Combined effect of NaCl-salinity and hypoxia on growth, photosynthesis, water relations and solute accumulation in *Phragmites australis* plants. *Flora* 205:462–470. <https://doi.org/10.1016/j.flora.2009.12.021>
- Guo Q, Hu Z, Li S, Hao Y, Liang N, Bai W, Zhang S (2021) Nitrogen-induced changes in carbon fluxes are modulated by water availability in a temperate grassland. *J Geophys Res: Biogeosci* 126:e2021JG006607. <https://doi.org/10.1029/2021JG006607>
- Han G, Chu X, Xing Q, Li D, Yu J, Luo Y, Wang G, Mao P, Rafique R (2015) Effects of episodic flooding on the net ecosystem CO₂ exchange of a supratidal wetland in the Yellow River. *Delta* 120:1506–1520. <https://doi.org/10.1002/2015JG002923>
- Hopple AM, Wilson RM, Kolton M, Zalman CA, Chanton JP, Kostka J, Hanson PJ, Keller JK, Bridgman SD (2020) Massive peatland carbon banks vulnerable to rising temperatures. *Nat Commun* 11:2373. <https://doi.org/10.1038/s41467-020-16311-8>
- Huang Y, Chen ZH, Tian B, Zhou C, Wang JT, Ge ZM, Tang JW (2020) Tidal effects on ecosystem CO₂ exchange in a *Phragmites* salt marsh of an intertidal shoal. *Agric For Meteorol* 292. <https://doi.org/10.1016/j.agrformet.2020.108108>
- Inglett KS, Inglett PW, Reddy KR, Osborne TZ (2012) Temperature sensitivity of greenhouse gas production in wetland soils of different vegetation. *Biogeochemistry* 108:77–90. <https://doi.org/10.1007/s10533-011-9573-3>
- Jiang X, Xie L, Ye S, Zhou P, Pei L, Chen H, Yu J, Zhao L (2022) Response of photosynthetic characteristics of *Phragmites australis* and *Spartina alterniflora* to the simulated warming in Jiangsu coastal wetlands (in Chinese with English abstract). *Acta Ecologica Sinica* 42:7760–7772. <https://doi.org/10.5846/stxb202106011444>
- Johnson CP, Pypker TG, Hribljan JA, Chimner RA (2013) Open Top Chambers and Infrared Lamps: a comparison of Heating Efficacy and CO₂/CH₄ Dynamics in a Northern Michigan Peatland. *Ecosystems* 16:736–748. <https://doi.org/10.1007/s10021-013-9646-3>
- Kaur H, Kaur H, Kaur H, Srivastava S (2022) The beneficial roles of trace and ultratrace elements in plants. *Plant Growth Regul.* <https://doi.org/10.1007/s10725-022-00837-6>
- Kroeger KD, Crooks S, Moseman-Valtierra S, Tang J (2017) Restoring tides to reduce methane emissions in impounded wetlands: a new and potent Blue Carbon climate change intervention. *Sci Rep* 7:11914. <https://doi.org/10.1038/s41598-017-12138-4>
- Lehmann A, Veresoglou SD, Leifheit EF, Rillig MC (2014) Arbuscular mycorrhizal influence on zinc nutrition in crop plants - a meta-analysis. *Soil Biol Biochem* 69:123–131. <https://doi.org/10.1016/j.soilbio.2013.11.001>
- Li C (2016) Biogeochemistry scientific fundamentals and modeling approach (in chinese). Tsinghua university press, Beijing China
- Li S-H, Ge Z-M, Xie L-N, Chen W, Yuan L, Wang D-Q, Li X-Z, Zhang L-Q (2018) Ecophysiological response of native and exotic salt marsh vegetation to waterlogging and salinity: implications for the effects of sea-level rise. *Sci Rep* 8:2441. <https://doi.org/10.1038/s41598-017-18721-z>
- Li Q, Gogo S, Leroy F, Guimbaud C, Laggoun-Défarge F (2021) Response of Peatland CO₂ and CH₄ fluxes to experimental warming and the Carbon Balance. 9. <https://doi.org/10.3389/feart.2021.631368>
- Liao CZ, Luo YQ, Jiang LF, Zhou XH, Wu XW, Fang CM, Chen JK, Li B (2007) Invasion of *Spartina alterniflora* enhanced ecosystem carbon and nitrogen stocks in the Yangtze Estuary. *China Ecosyst* 10:1351–1361. <https://doi.org/10.1007/s10021-007-9103-2>
- Liu J-q, Wang W-q, Shen L-d, Yang Y-l, Xu J-b, Tian M-h, Liu X, Yang W-t, Jin J-h, Wu H-s (2022) Response of methanotrophic activity and community structure to plant invasion in China's coastal wetlands. *Geoderma* 407:115569. <https://doi.org/10.1016/j.geoderma.2021.115569>
- Liu J, Ye SY, Laws EA, Xue CT, Yuan HM, Ding XG, Zhao GM, Yang SX, He L, Wang J, Pei SF, Wang YB, Lu QY (2017) Sedimentary environment evolution and biogenic silica records over 33,000 years in the Liaohe delta,

- China. *Limnol Oceanogr* 62:474–489. <https://doi.org/10.1002/lno.10435>
- Lo Iacono C, Mateo MA, Gracia E, Guasch L, Carbonell R, Serrano L, Serrano O, Danobeitia J (2008) Very high-resolution seismo-acoustic imaging of seagrass meadows (Mediterranean Sea): implications for carbon sink estimates. *Geophys Res Lett* 35:L18601. <https://doi.org/10.1029/2008gl034773>
- Lu QY, Pei LX, Ye SY, Laws EA, Brix H (2020) Negative feedback by vegetation on soil organic matter decomposition in a coastal wetland. *Wetlands* 40:2785–2797. <https://doi.org/10.1007/s13157-020-01350-0>
- Macreadie PI, Hughes AR, Kimbro DL (2013) Loss of ‘blue carbon’ from coastal salt marshes following habitat disturbance. *PLoS ONE* 8:e69244. <https://doi.org/10.1371/journal.pone.0069244>
- Mahecha MD, Reichstein M, Carvalhais N, Lasslop G, Lange H, Seneviratne SI, Vargas R, Ammann C, Arain MA, Cescatti A, Janssens IA, Migliavacca M, Montagnani L, Richardson AD (2010) Global convergence in the temperature sensitivity of respiration at Ecosystem Level. *Science* 329:838–840. <https://doi.org/10.1126/science.1189587>
- McKee KL, Cahoon DR, Feller IC (2007) Caribbean mangroves adjust to rising sea level through biotic controls on change in soil elevation. *Glob Ecol Biogeogr* 16:545–556. <https://doi.org/10.1111/j.1466-8238.2007.00317.x>
- McLennan SM (1993) Weathering and global denudation. *J Geol* 101:295–303. <https://doi.org/10.1086/648222>
- Mueller P, Hager RN, Meschter JE, Mozdzer TJ, Langley JA, Jensen K, Megonigal JP (2016) Complex invader-ecosystem interactions and seasonality mediate the impact of non-native Phragmites on CH₄ emissions. *Biol Invasions* 18:2635–2647. <https://doi.org/10.1007/s10530-016-1093-6>
- Munir TM, Strack M (2014) Methane Flux Influenced by Experimental Water table drawdown and soil warming in a dry Boreal Continental Bog. *Ecosystems* 17:1271–1285. <https://doi.org/10.1007/s10021-014-9795-z>
- Nellemann C, Corcoran E, Duarte CM, Valdés L, DeYoung C, Fonseca LE, Grimsditch GD (2009) Blue carbon - a rapid response assessment. Environment. United Nations Environment Programme. GRID-Arendal. <https://www.grida.no>
- Nesbitt HW, Young GM (1982) Early proterozoic climates and plate motions inferred from major element chemistry of lutites. *Nature* 299:715–717. <https://doi.org/10.1038/299715a0>
- Neubauer SC (2021) Global warming potential is not an ecosystem property. *Ecosystems* 24:2079–2089. <https://doi.org/10.1007/s10021-021-00631-x>
- Neubauer SC, Megonigal JP (2015) Moving beyond global warming potentials to quantify the climatic role of Ecosystems. *Ecosystems* 18:1000–1013. <https://doi.org/10.1007/s10021-015-9879-4>
- Neubauer SC, Megonigal JP (2019) Moving beyond global warming potentials to quantify the climatic role of ecosystems (vol 18, pg 1000, 2015). *Ecosystems* 22:1931–1932. <https://doi.org/10.1007/s10021-019-00422-5>
- Neubauer SC, Megonigal JP (2021) Biogeochemistry of wetland carbon preservation and flux. *Wetland Carbon Environ Manag*. <https://doi.org/10.1002/9781119639305.ch3>
- Noyce GL, Megonigal JP (2021) Biogeochemical and plant trait mechanisms drive enhanced methane emissions in response to whole-ecosystem warming. *Biogeosciences* 18:2449–2463. <https://doi.org/10.5194/bg-18-2449-2021>
- Oberbauer SF, Tweedie CE, Welker JM, Fahnestock JT, Henry GHR, Webber PJ, Hollister RD, Walker MD, Kuchy A, Elmore E, Starr G (2007) Tundra CO₂ fluxes in response to experimental warming across latitudinal and moisture gradients. *Ecol Monogr* 77:221–238. <https://doi.org/10.1890/06-0649>
- Olsson L, Ye S, Yu X, Wei M, Krauss KW, Brix H (2015) Factors influencing CO₂ and CH₄ emissions from coastal wetlands in the Liaohe delta, Northeast China. *Biogeosciences* 12:4965–4977. <https://doi.org/10.5194/bg-12-4965-2015>
- Pagter M, Bragato C, Malagoli M, Brix H (2009) Osmotic and ionic effects of NaCl and Na₂SO₄ salinity on phragmites australis. *Aquat Bot* 90:43–51. <https://doi.org/10.1016/j.aquabot.2008.05.005>
- Parida AK, Das AB (2005) Salt tolerance and salinity effects on plants: a review. *Ecotoxicol Environ Saf* 60:324–349. <https://doi.org/10.1016/j.ecoenv.2004.06.010>
- Pearson M, Penttila T, Harjunpaa L, Laiho R, Laine J, Sarjala T, Silvan K, Silvan N (2015) Effects of temperature rise and water-table-level drawdown on greenhouse gas fluxes of boreal sedge fens. *Boreal Environ Res* 20:489–505
- Pierfelice KN, Lockaby BG, Krauss KW, Conner WH, Noe GB, Ricker MC (2017) Salinity influences on Aboveground and Belowground Net Primary Productivity in Tidal Wetlands. *J Hydrol Eng* 22. [https://doi.org/10.1061/\(asce\)he.1943-5584.0001223](https://doi.org/10.1061/(asce)he.1943-5584.0001223)
- Poffenbarger HJ, Needelman BA, Megonigal JP (2011) Salinity influence on methane emissions from tidal marshes. *Wetlands* 31:831–842. <https://doi.org/10.1007/s13157-011-0197-0>
- Portnoy JW (1999) Salt marsh diking and restoration: biogeochemical implications of altered Wetland Hydrology. *Environ Manage* 24:111–120. <https://doi.org/10.1007/s002679900219>
- Ravn NR, Michelsen A, Reboleira ASP (2020) Decomposition of organic matter in caves. *Front Ecol Evol* 8:554651. <https://doi.org/10.3389/fevo.2020.554651>
- Rumpel C, Kögel-Knabner I (2011) Deep soil organic matter—a key but poorly understood component of terrestrial C cycle. *Plant Soil* 338:143–158. <https://doi.org/10.1007/s11104-010-0391-5>
- Tan L-S, Ge Z-M, Li S-H, Li Y-L, Xie L-N, Tang J-W (2021) Reclamation-induced tidal restriction increases dissolved carbon and greenhouse gases diffusive fluxes in salt marsh creeks. *Sci Total Environ* 773:145684. <https://doi.org/10.1016/j.scitotenv.2021.145684>
- Thongbai P, Kozai T, Ohshima K (2010) CO₂ and air circulation effects on photosynthesis and transpiration of tomato seedlings. *Sci Hort* 126:338–344. <https://doi.org/10.1016/j.scienta.2010.07.018>
- Tong C, Wang W-Q, Huang J-F, Gauci V, Zhang L-H, Zeng C-S (2012) Invasive alien plants increase CH₄ emissions from a subtropical tidal estuarine wetland. *Biogeochemistry* 111:677–693. <https://doi.org/10.1007/s10533-012-9712-5>

- Touchette BW, Steudler SE (2009) Climate change, drought, and wetland vegetation. In: E Nzewi, G Reddy, S Luster-Teasley, V Kabadi, S-Y Chang, K Schimmel, G Uzochukwu (eds) Proceedings of the 2007 National Conference on Environmental Science and Technology. Springer New York, New York, NY. https://doi.org/10.1007/978-0-387-88483-7_32
- USEPA-United States Environmental Protection Agency (2020) Tidal restriction synthesis review: an analysis of U.S. tidal restrictions and opportunities for their avoidance and removal. Washington D.C. Document No. EPA-842-R-20001
- Volik O, Petrone RM, Quanz M, Macrae ML, Rooney R, Price JS (2020) Environmental controls on CO₂ exchange along a salinity gradient in a saline boreal fen in the Athabasca Oil Sands Region. *Wetlands* 40:1353–1366. <https://doi.org/10.1007/s13157-019-01257-5>
- Wang W, Sardans J, Wang C, Zeng C, Tong C, Chen G, Huang J, Pan H, Peguero G, Vallicrosa H, Peñuelas J (2019) The response of stocks of C, N, and P to plant invasion in the coastal wetlands of China. *Glob Change Biol* 25:733–743. <https://doi.org/10.1111/gcb.14491>
- Wei S, Han G, Chu X, Song W, He W, Xia J, Wu H (2020) Effect of tidal flooding on ecosystem CO₂ and CH₄ fluxes in a salt marsh in the Yellow River Delta. *Estuar Coast Shelf Sci* 232:106512. <https://doi.org/10.1016/j.ecss.2019.106512>
- Xu X, Fu G, Zou X, Ge C, Zhao Y (2017) Diurnal variations of carbon dioxide, methane, and nitrous oxide fluxes from invasive *Spartina alterniflora* dominated coastal wetland in northern Jiangsu Province. *Acta Oceanol Sin* 36:105–113. <https://doi.org/10.1007/s13131-017-1015-1>
- Xu X, Wei S, Chen H, Li B, Nie M (2022) Effects of *Spartina* invasion on the soil organic carbon content in salt marsh and mangrove ecosystems in China. *J Appl Ecol* 59:1937–1946. <https://doi.org/10.1111/1365-2664.14202>
- Xu XW, Zou XQ, Cao LG, Zhamangulova N, Zhao YF, Tang DH, Liu DW (2014) Seasonal and spatial dynamics of greenhouse gas emissions under various vegetation covers in a coastal saline wetland in southeast China. *Ecol Eng* 73:469–477. <https://doi.org/10.1016/j.ecoleng.2014.09.087>
- Yan N, Marschner P (2013) Response of soil respiration and microbial biomass to changing EC in saline soils. *Soil Biol Biochem* 65:322–328. <https://doi.org/10.1016/j.soilbio.2013.06.008>
- Yang P, Lai DYF, Huang JF, Zhang LH, Tong C (2018) Temporal variations and temperature sensitivity of ecosystem respiration in three brackish marsh communities in the Min River Estuary, southeast China. *Geoderma* 327:138–150. <https://doi.org/10.1016/j.geoderma.2018.05.005>
- Ye S, Laws EA, Yuknis N, Ding X, Yuan H, Zhao G, Wang J, Yu X, Pei S, DeLaune RD (2015) Carbon sequestration and soil accretion in coastal wetland communities of the yellow river delta and Liaohe Delta, China. *Estuaries Coasts* 38:1885–1897. <https://doi.org/10.1007/s12237-014-9927-x>
- Ye S, Krauss KW, Brix H, Wei M, Olsson L, Yu X, Ma X, Wang J, Yuan H, Zhao G, Ding X, Moss RF (2016) Inter-annual variability of area-scaled gaseous carbon emissions from wetland soils in the Liaohe Delta, China. *PLoS One* 11:e0160612. <https://doi.org/10.1371/journal.pone.0160612>
- Ye SY, Xie LJ, He L (2021) Wetlands-the kidney of the Earth & a Boat of Life. China Science Publishing & Media Ltd. (CSPM), Bei Jing
- Yu X, Ye S, Pei L, Xie L, Krauss K, Chapman S, Brix H (2023) Biophysical warming patterns of an open-top chamber and its short-term influence on a *Phragmites* wetland ecosystem in China. *China Geol* 1–17. <https://doi.org/10.31035/cg2022064>
- Yu J, Zhou D, Han G, Guan B (2018) Biogeochemical processes of nutrient elements in Coastal Wetland of the Yellow River Delta. China Science Publishing & Media Ltd. (CSPM), Beijing China
- Yuan J, Ding W, Liu D, Kang H, Freeman C, Xiang J, Lin Y (2015) Exotic *Spartina alterniflora* invasion alters ecosystem-atmosphere exchange of CH₄ and N₂O and carbon sequestration in a coastal salt marsh in China. *Glob Change Biol* 21:1567–1580. <https://doi.org/10.1111/gcb.12797>
- Zhang Y, Ding W, Cai Z, Valerie P, Han F (2010a) Response of methane emission to invasion of *Spartina alterniflora* and exogenous N deposition in the coastal salt marsh. *Atmos Environ* 44:4588–4594. <https://doi.org/10.1016/j.atmosenv.2010.08.012>
- Zhang Y, Ding W, Luo J, Donnison A (2010b) Changes in soil organic carbon dynamics in an eastern chinese coastal wetland following invasion by a C4 plant *Spartina alterniflora*. *Soil Biol Biochem* 42:1712–1720. <https://doi.org/10.1016/j.soilbio.2010.06.006>
- Zhao ML, Han GX, Li JY, Song WM, Qu WD, Eller F, Wang JP, Jiang CS (2020) Responses of soil CO₂ and CH₄ emissions to changing water table level in a coastal wetland. *J Clean Prod* 269. <https://doi.org/10.1016/j.jclepro.2020.122316>
- Zhao G, Ye S, Yuan H, Ding X, Wang J, Laws EA (2018) Surface sediment properties and heavy metal contamination assessment in river sediments of the Pearl River Delta, China. *Mar Pollut Bull* 136:300–308. <https://doi.org/10.1016/j.marpolbul.2018.09.035>
- Zhou C, Zhao H, Sun Z, Zhou L, Fang C, Xiao Y, Deng Z, Zhi Y, Zhao Y, An S (2015) The invasion of *Spartina alterniflora* alters carbon dynamics in China's Yancheng natural reserve. *CLEAN – Soil. Air Water* 43:159–165. <https://doi.org/10.1002/clen.201300839>

Publisher's note Springer Nature remains neutral with regard to jurisdictional claims in published maps and institutional affiliations.

Springer Nature or its licensor (e.g. a society or other partner) holds exclusive rights to this article under a publishing agreement with the author(s) or other rightsholder(s); author self-archiving of the accepted manuscript version of this article is solely governed by the terms of such publishing agreement and applicable law.